AD-A061 824 ROYAL AIRCRAFT ESTABLISHMENT FARNBOROUGH (ENGLAND) F/G 22/3
COSMOS 462 (1971-106A): ORBIT DETERMINATION AND ANALYSIS.(U)
AUG 78 D M WALKER
UNCLASSIFIED RAE-TR-78089 DRIC-BR-64935 NL

1 OF 1
AD
A061824

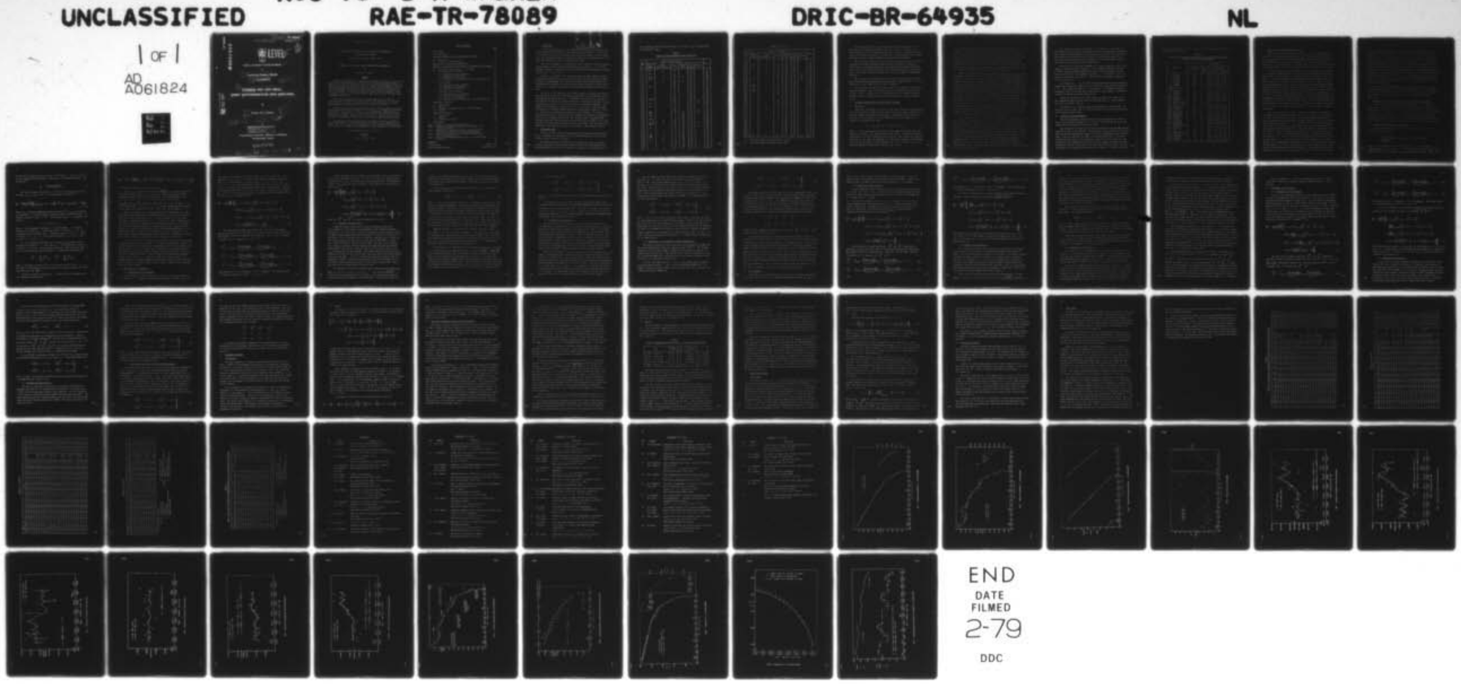

END
DATE
FILMED
2-79
DDC

TR 78089

AD A061824

(14) RAE-TR-78089

UNLIMITED

BR64935

(1)

LEVEL II

ROYAL AIRCRAFT ESTABLISHMENT

*

(9) Technical Report 78089

(11) August 1978

(12) 63p.

(6) COSMOS 462 (1971-106A): ORBIT DETERMINATION AND ANALYSIS.

by

(10) Doreen M.C. Walker

(18) DRIC (19) BR-64935

*

Procurement Executive, Ministry of Defence

Farnborough, Hants

UNLIMITED

310 450 78 11 22 038

UDC 629.19.077.3 : 521.6

ROYAL AIRCRAFT ESTABLISHMENT

Technical Report 78089

Received for printing 8 August 1978

COSMOS 462 (1971-106A): ORBIT DETERMINATION AND ANALYSIS

by

Doreen M. C. Walker

Summary

Cosmos 462 (1971-106A) was launched on 3 December 1971 into an orbit inclined at 65.75° to the equator, with a perigee height of 230 km and apogee height of 1800 km. The satellite remained in orbit for 40 months and decayed on 4 April 1975. Orbital parameters have been determined at 85 epochs, using the RAE orbit refinement program, PROP, with 6635 radar and optical observations, including 197 from the Hewitt cameras. The average standard deviation in eccentricity and inclination corresponded to a positional accuracy of about 100 m. In addition, orbits of similar accuracy were determined daily for the last 15 days of the life, from 2000 NORAD observations.

During its slow decay, the orbit passed through 14:1, 29:2 and 15:1 resonances with the Earth's gravitational field. The variations in inclination and eccentricity at these resonances have been analysed in detail to evaluate lumped geopotential harmonic coefficients of order 14, 29 and 15.

The variation of inclination between resonances has been analysed to obtain four values of the average atmospheric rotation rate Λ at heights of 200-250 km in 1972-1975. The values of Λ show a seasonal dependence, being greater in winter than in summer, and the average rotation rate is lower than in the 1960s, being near 1.0 rev/day. Analysis of the inclination in the last 15 days of the satellite's life indicates a weak west-to-east wind at high latitude (54-62°N).

The variation of perigee height has been analysed to obtain 24 values of density scale height H, including eight in the last 15 days. Comparison with values from *CIRA 1972* shows a bias difference of only 1% and rms difference of 10%; so *CIRA 1972* provides a good approximation to the values of H in 1972-1975.

Departmental Reference: Space 555

LIST OF CONTENTS

089

1 INTRODUCTION

Cosmos 462 entered orbit on 3 December 1971 and was one of a pair of satellites launched by the Russians to test high-speed interception[1-3]. Cosmos 462 was the hunter satellite and exploded after passing the target satellite, Cosmos 459. This explosion occurred 3.5 hours after launch and the largest piece of the satellite remaining in orbit was designated 1971-106A.

After this experiment, 1971-106A had an orbital period of about 105 minutes, perigee height 230 km, apogee height 1800 km and inclination, i, 65.7°; the satellite remained in orbit for 40 months, without further disturbance, and decayed naturally on 1975 April 4.90[4].

Early in its lifetime, 1971-106A was selected for high-priority observing by the British optical and radar tracking stations, including the Hewitt cameras at Malvern and Edinburgh; 1971-106A was in an orbit which would be useful for determining the atmospheric rotational speed from the decrease in orbital inclination, and air density at heights near 200 km could be evaluated from its decay rate.

The orbit of 1971-106A has been determined from all available observations with the aid of the RAE orbit refinement program PROP[5], in the PROP6 version[6], at 85 epochs during its 40-month life. In addition 15 daily orbits at the end of the life were determined from NORAD observations. This Report describes the orbit determinations, and the analyses of variations in the orbital parameters. The changes in inclination and eccentricity at 14:1, 29:2 and 15:1 resonances have been analysed to determine lumped geopotential coefficients of order 14, 29 and 15. (There was no detectable perturbation at 31:2 resonance.) The values of inclination between the resonances have been analysed to determine the atmospheric rotation rate at heights near 200 km. The accurate values of perigee height obtained, which have already been used in evaluating the air density[7], have been analysed to determine the atmospheric density scale height. The residuals of the observations have been used to assess the accuracy of each observing station.

2 THE OBSERVATIONS

The orbit of 1971-106A has been determined at 85 epochs from 6635 observations. A breakdown of the number and type of observations used on each of the 85 runs is given in Table 1 on page 4.

The observations can be divided into six groups (see Table 1), the most
089 accurate being those from the Hewitt cameras at Malvern (M) and Edinburgh (E).
These observations, which were available on 43 transits, 29 from Malvern and 14

from Edinburgh, usually have an accuracy of *2 seconds of arc in position* and 1 millisecond in time.

Table 1

Sources of the observations used in each run

Run No.	Source of observations						Total
	Hewitt camera	Cape kinetheodolite	Visual	British radar	US Navy	Finland	
1	10E	4	11		29		54
2		6	5		38		49
3	15M		41		31		87
4		4	35		47		86
5	5E,4M	2	37	6	26		80
6	1M		39		15		55
7		2	20	15	39		76
8			28		30		58
9			46		25		71
10	5M		10		36		51
11			21		47		68
12			2		34		36
13			10		56		66
14			13		76		89
15			15	5	46		66
16			35		36		71
17	5E,7M		43		40		95
18			35		34	29	98
19	4E		23		56	5	88
20		2	3		34		39
21	10E		14		53		77
22			15		35		50
23			43		45	3	91
24	10M		26	17	40	18	111
25	10E		7	38	29		84
26	5M		5	38	25		73
27			3	46	33		82
28	5M,5E		9	50	32		101
29		12	18	36	24		90
30	15E,15M	2	51	16	2	3	104
31	5M		41	12	18		76
32			26	44	18	16	104
33	5M		5	40	17		67
34			9	34	22		65
35		6	9	21	28		64
36	5M		17	20	22		64
37	6M	8	9	18	21		62
38	10M		3	46	33		92
39		14	14	30	18		76
40	5E		3	17	26		51
41		6	10	10	35		61
42			6	33	22		61
43			11	36	27	4	78
44		16	37	24	25	3	105

Table 1 (concluded)

Run No.	Source of observations						Total
	Hewitt camera	Cape kinetheodolite	Visual	British radar	US Navy	Finland	
45		4	7	34	26		71
46		4	3	35	30		72
47		2	4	36	25		67
48	5M		32	30	31		98
49		8	39	40	31		118
50			4	48	41		93
51			7	44	32		83
52		4	6	28	23	3	64
53			44	24	16	9	93
54		2	16	36	28	12	94
55	5M		21	30	39	15	110
56			24	36	35		95
57				35	43		78
58			13	39	35		87
59	10M		13	36	36		95
60		2	13	50	32		97
61	5M		24	48	41		118
62	5M		12	36	24		77
63			48	42	34		124
64			9	54	32		95
65				31	33		64
66			4	42	27		73
67			10	44	33		87
68			25	50	33		108
69			11	40	34		85
70		2	10	48	31		91
71		2	3	58	30		93
72		6	6	44	23		79
73			13	42	28		83
74			4	44	29		77
75			4	52	17		73
76			2	56	18		76
77		4	5	66	25		100
78			2	52	20		74
79				56	21		77
80			4	50	17		71
81		2		36	24		62
82				34	10		44
83				28	17		45
84				8	13		21
85				41	10		51
Total	197	126	1305	2335	2552	120	6635

E = observations made by Edinburgh Hewitt camera

M = observations made by Malvern Hewitt camera

The observations in the second group, made by the kinetheodolite at the South African Astronomical Observatory, have an accuracy of 1 minute of arc. These observations are very valuable because they can greatly improve the orbital accuracy, especially the values of eccentricity, as they are made in the southern hemisphere, whereas northern-hemisphere observations are predominant.

The third group consists of visual observations made by volunteer observers reporting to the Radio and Space Research Station (now Appleton Laboratory), Slough, and to the Moonwatch Division of the Smithsonian Astrophysical Observatory. These visual observations usually have accuracies between 1 and 4 minutes of arc. This group accounted for about 20% of the total number of observations available.

The fourth group of observations are those made by British radar stations. About 80 observations were made by the radar tracker at RRE, Malvern, and the rest, around 2250, by the radar trackers at RAF, Fylingdales.

The fifth group consists of US Navy observations, supplied by the US Naval Research Laboratory. Some 2550 observations were available with a topocentric accuracy of about 2 minutes of arc. The final group of 120 observations comes from the theodolite at Jokioinen, Finland, with accuracies of about 5 minutes of arc.

3 THE ORBITS OBTAINED AND THE OBSERVATIONAL ACCURACY

3.1 The orbits

Orbits were determined at 85 epochs fairly evenly spaced over the satellite's life, and the orbital elements at each epoch are listed in Table 2 on pages 38-41 with the standard deviations below each value. The epoch for each orbit is at 00 hours on the day indicated. In the PROP6 model[6] the mean anomaly M is fitted by a polynomial of the form

$$M = M_0 + M_1 t + M_2 t^2 + M_3 t^3 + M_4 t^4 + M_5 t^5 , \qquad (1)$$

where t is the time measured from epoch and the number of M-coefficients used depends on the drag. For a high-drag orbit like that of 1971-106A, the number of coefficients to be used is found by trial and error. Best results were obtained using M_0 to M_5, the full complement of coefficients allowed in the PROP model, for 32 of the 85 orbits; 33 orbits required M_0 to M_4; 16 orbits M_0 to M_3 and the remaining 4 needed only coefficients M_0 to M_2. 089

The orbits all fit the observations in a satisfactory manner, with ε, the parameter indicating the measure of fit, ranging between 0.99 and 0.30, where ε^2 is the sum of the squares of the weighted residuals divided by the number of degrees of freedom; and the weighted residual is defined as the value (of right ascension or declination) given by the orbit, minus the value given by the observation, divided by the *a priori* error assigned to the observation. No particular difficulty in fitting was experienced at the times of magnetic storms, when the drag is liable to vary irregularly. For example, the orbit at the time of the major solar disturbance in early August 1972 fitted well.

Hewitt camera observations were available for inclusion in 24 of the orbits determined, see Tables 1 and 2. For these 24 orbits the standard deviation in eccentricity ranged from 0.000002 to 0.000029 with an average of 0.000012, corresponding to about 80 m in perigee or apogee height. The standard deviations in inclination varied from 0.0001° to 0.0011° giving an average sd of 0.0006°, also equivalent to about 80 m in distance. The other 61 orbits, those without Hewitt camera observations, had standard deviations in inclination varying from 0.0007° to 0.0030° with an average of 0.0014°, equivalent to some 170 m in distance, more than double the average sd of the orbits with Hewitt camera observations. The improvement in accuracy for eccentricity is less significant, being about 15%. The same increase in accuracy for eccentricity is achieved on those orbits using the Cape kinetheodolite observations. This confirms the opinion already expressed that, while the Hewitt camera observations greatly improve the accuracy of the orbital inclination (and the other orbital parameters to a lesser degree), the southern hemisphere observations have a great influence in defining the shape of the orbit, as shown by the increased accuracy in eccentricity.

Fig 1 shows the values of eccentricity, from Table 2: the gradual decrease due to drag is the dominant feature; for most satellites the oscillation due to odd zonal harmonics is usually also important, but it is so small as to be imperceptible for 1971-106A, because the inclination (65.7°) is close to the value (66.1°) where the effect of the third zonal harmonic is cancelled by the effects of the fifth and higher harmonics (see Ref 8). The maxima and minima in slope of the curve in Fig 1 coincide with the minima and maxima in the variation of the satellite's perigee height, which occur when the perigee is at the equator or at maximum latitude. Fig 4 of Ref 7 shows that perigee height has maxima at MJD 41575, 41920 and 42240, and minima at MJD 41410, 41760, 42105 amd 42420. (The triangles in Fig 1 indicate values from the daily orbits for the last 15 days of the life, see section 4.)

Fig 2 shows the values of inclination, i, from Table 2 (and Table 4). These values of inclination are irregular, and before any meaningful conclusions can be drawn from the variation of inclination, the values must be cleared of all perturbations (see sections 5 and 6). However, the perturbing effects of the 14th- and 15th-order resonances are discernible in the observational values, at dates centred on MJD 41659 and 42302 respectively.

The accuracy of other orbital parameters is much as expected. Most of the values of right ascension of the node, Ω, have standard deviations of 0.001° or 0.002°, generally slightly higher than the sd in the inclination. In the first half of the life, the argument of perigee, ω, is accurate to 0.01°, but as usual the sd tends to vary as e^{-1} and increases considerably towards the end of the life as $e \to 0$.

The variation of ω for 1971-106A is much slower than for most satellites, because the inclination is quite close to the critical value of 63.4°, for which $\dot{\omega} = 0$. Fig 3 shows the values of ω from Table 2: the argument of perigee decreases by about $\frac{1}{2}^{\circ}$ per day, and perigee does not quite complete 2 revolutions during the 40 months of the satellite's life.

Nearly all the values of M_1, are accurate to better than 1 part in 10^6, and consequently nearly all the values of semi major axis, a, have standard deviations of between 1 and 3 m.

The values of M_2, which provide a direct measure of the air drag[7], are mostly accurate to better than $\frac{1}{2}$%: they are plotted in Fig 4 and have been fully utilized and discussed in Ref 7.

3.2 Accuracy of the observations

The orbit refinement program proceeds by rejecting observations which do not fit well (weighted residuals $>3\varepsilon$): a total of 5449 observations out of the original 6635 were accepted in the final orbits.

The residuals of the observations have been obtained using the ORES computer program[9] and sent to the observers. The accuracies of selected observing stations, with five or more observations accepted in the orbit determination, are listed in Table 3, page 9, along with the number of accepted observations. The US Navy observations from station 29 are geocentric, and if they were given in the same form as the other (topocentric) observations, their angular rms residuals would increase by a factor of about five. The total rms residuals in Table 3 are much as expected: 0.04 minutes of arc for the Hewitt cameras; 1.3 minutes of arc for 089 the Cape kinetheodolite; and from 2.0 minutes of arc upwards for the visual observers and theodolites.

Table 3

Residuals for observing stations with more than five observations accepted in the orbit determination

Station		Number of observations accepted	Rms residuals			
			Range km	Minutes of arc		
				RA	Dec	Total
1	US Navy	245		1.9	2.0	2.8
2	US Navy	104		1.9	2.0	2.8
3	US Navy	103		1.5	1.5	2.1
4	US Navy	110		1.6	1.5	2.2
5	US Navy	154		1.7	1.6	2.3
6	US Navy	185		1.8	1.8	2.5
29	US Navy	1275	0.6	0.3	0.4	
81, 2594	Londerzeel	7		1.5	1.3	2.0
414	Capetown	89		3.2	3.4	4.7
725	Bucharest	7		4.0	6.2	7.4
1114	Miskolc	10		3.3	2.9	4.4
1963	Jokioinen	109		3.7	3.0	4.7
2265	Farnham	35		2.1	2.0	2.9
2303	Malvern Hewitt camera	106		0.03	0.03	0.04
2304	Malvern radar	78	1.3	2.0	2.5	
2406	Dublin	7		2.2	2.7	3.5
2414	Bournemouth	168		4.0	4.2	5.8
2419	Tremadoc	35		2.6	2.7	3.7
2420	Willowbrae	227		2.2	2.2	3.1
2421	Malvern 4	159		1.7	1.7	2.4
2430	Stevenage 4	14		1.8	1.5	2.3
2437	Warrington	7		3.9	4.7	6.1
2502	Sudbury	6		6.0	5.8	8.3
2513	Colchester	7		4.9	10.1	11.2
2528	Aldershot	7		1.7	1.6	2.3
2534	Edinburgh Hewitt camera	51		0.03	0.02	0.04
2539	Dymchurch	7		1.3	1.8	2.3
2550	Masirah	22		1.6	2.2	2.7
2577	Cape kinetheodolite	89		0.9	1.0	1.3
2596	Akrotiri	40		3.1	3.9	5.0
4126	Groningen	13		2.6	2.3	3.5
4130	Denekamp	8		3.7	4.4	5.7
8597	Adelaide	16		2.2	3.1	3.8

089

4 ORBITS FOR THE FIFTEEN DAYS BEFORE DECAY

After the orbital determinations described in section 3 were completed, a further 2000 observations were provided by the assigned and contributing sensors of the North American Air Defense Command (NORAD) Space Detection and Tracking System (SPADATS) for the last 15 days before decay. With the aid of these observations it has been possible to determine orbits at the end of the satellite's life more accurately and at closer intervals than has been possible in the past.

Fifteen further orbits were determined at daily intervals from 1975 March 21.0, using these NORAD observations together with other observations previously used in orbits 83-85 of Table 2. The orbital elements are listed in Table 4 on page 42, with the standard deviations below each value. As before, the epoch for each orbit is at 00 hours on the day indicated. In 11 of these 15 orbits, only the coefficients M_0, M_1 and M_2 were required in the polynomial for mean anomaly, equation (1). This is unusual, because the full set of coefficients is generally needed near decay (as in Table 2): here, however, the observations for each orbit extend over no more than 24 hours, so that $t \lesssim 0.5$ and terms in t^3, t^4 and t^5 have much less effect than when $t > 1$ as for the orbits of Table 2. For example, if the set of coefficients in orbit 84 of Table 2 were correct, the value of $M_4 t^4 (= 0.05t^4)$ would be $<0.003^o$ for $t < 0.5$. So the term would not be significant for the one-day orbit, and M_4 would not be needed. The values of e, i and M_2 from Table 4 have been added at the end of Figs 1, 2 and 4 respectively.

The last three orbits in Table 2 (orbits 83, 84 and 85) are virtually independent of the corresponding orbits in Table 4 (orbits E, J and N), because the latter orbits include only a few of the original observations, which are greatly outweighed by the large number of NORAD observations. So it is interesting to compare the elements. *Orbit 83* is based on only 30 observations spread over 5.9 days, and requires all six M-coefficients, so that 10 parameters are being determined from 30 observations. This might almost be called a recipe for unreliability. The corresponding one-day orbit, E, with 78 observations and only M_0, M_1 and M_2, should be much more reliable. Comparison shows that the values of e, Ω and M_2 in orbit 83 are inconsistent with those of orbit E, but the values of i, ω, M_0 and M_1 are within the combined sd. So orbit 83 emerges from the comparison surprisingly well. *Orbit 84* is based on only 16 observations spread over 2.9 days, and requires five M-coefficients, so that 9 parameters are being determined from 16 observations. This might seem likely to be 089
disastrous, and it is not surprising that the sd in inclination is the largest

among the 85 orbits. Comparison with the more accurate and more reliable orbit J shows that, although the values of i and M_2 differ significantly, the values of e, Ω, $(\omega + M_0)$ and M_1 are consistent. So orbit 84, though potentially disastrous, is fairly reliable. *Orbit 85* has 39 observations and covers 2.5 days before decay: six M-coefficients are needed and M_2 is exceptionally large (8.6 deg/day^2). All analytical orbit determination programs break down at decay because the perturbations become unlimited, so orbit 85 must inevitably be looked on with suspicion. Comparison with orbit N shows some significant differences, twice the sum of the sd on inclination and five times on eccentricity, but good agreement on Ω and $(\omega + M_0)$. So, although the last three orbits of Table 2 were all potentially bad (through lack of observations and proximity to decay), they emerge remarkably well from the test of comparison with the (more accurate) one-day orbits.

On average the standard deviations on orbits 83-85 of Table 2 are about three times larger than on the corresponding one-day orbits. The accuracy of the one-day orbits is somewhat better than those of the main orbits without Hewitt camera observations, though not so good as the orbits with Hewitt camera observations.

5 ANALYSIS OF VARIATION IN INCLINATION AND ECCENTRICITY AT RESONANCE

If we accept the assumption that the geopotential can be expanded in a double infinite series of tesseral harmonics, 'lumped' harmonic coefficients of a particular order (linear functions of individual coefficients) can be determined by analysing the changes that occur in the orbital elements of satellites which experience resonance of that order. The satellite 1971-106A was appreciably perturbed on passing through 14:1, 29:2 and 15:1 resonances, and the effects of these resonances on the orbital inclination and eccentricity have been evaluated.

5.1 Theoretical equations for $\beta:\alpha$ resonance

The longitude-dependent geopotential at an exterior point (r, θ, λ) may be written in normalized form[10] as

$$\frac{\mu}{r}\sum_{\ell=2}^{\infty}\sum_{m=1}^{\ell}\left(\frac{R}{r}\right)^{\ell}P_{\ell}^{m}(\cos\theta)\left\{\bar{C}_{\ell m}\cos m\lambda + \bar{S}_{\ell m}\sin m\lambda\right\}N_{\ell m}\,, \qquad (2)$$

where r is the distance from the Earth's centre, θ is co-latitude, λ is
089 longitude (positive to the east), μ is the gravitational constant for the Earth (398601 km^3/s^2), R is the Earth's equatorial radius (6378.1 km), $P_{\ell}^{m}(\cos\theta)$ is

the associated Legendre function of order m and degree ℓ, and $\bar{C}_{\ell m}$ and $\bar{S}_{\ell m}$ are the normalized tesseral harmonic coefficients. The normalizing factor $N_{\ell m}$ is given by[10]

$$N_{\ell m}^2 = \frac{2(2\ell + 1)(\ell - m)!}{(\ell + m)!} \ . \tag{3}$$

The rate of change of inclination i caused by a relevant pair of coefficients, $\bar{C}_{\ell m}$ and $\bar{S}_{\ell m}$, near $\beta{:}\alpha$ resonance may be written[11,12]

$$\frac{di}{dt} = \frac{n(1 - e^2)^{-\frac{1}{2}}}{\sin i}\left(\frac{R}{a}\right)^{\ell} \bar{F}_{\ell mp} G_{\ell pq}(k \cos i - m)\mathscr{R}\left[j^{\ell - m + 1}(\bar{C}_{\ell m} - j\bar{S}_{\ell m})\exp\{j(\gamma\Phi - q\omega)\}\right] , \qquad \ldots\ldots (4)$$

where $\bar{F}_{\ell mp}$ is Allan's normalized inclination function[12], $G_{\ell pq}$ is a function of eccentricity e for which explicit forms have been derived by Gooding[11], $\mathscr{R}$ denotes 'real part of' and $j = \sqrt{-1}$. The resonance angle Φ is defined by the equation

$$\Phi = \alpha(\omega + M) + \beta(\Omega - \nu) \ , \tag{5}$$

where ω is the argument of perigee, M the mean anomaly, Ω the right ascension of the node and ν the sidereal angle. The indices γ, q, k and p in equation (3) are integers, with γ taking the values 1, 2, 3 ...... and q the values 0, ±1, ±2, ... ; the equations linking ℓ, m, k and p are[11]: $m = \gamma\beta$; $k = \gamma\alpha - q$; $2p = \ell - k$.

At $\beta{:}\alpha$ resonance the m-suffix of a relevant $(\bar{C}_{\ell m}, \bar{S}_{\ell m})$ pair is given uniquely by the choice of γ . The values of ℓ to be taken must be such that $\ell \geqslant m$ and $(\ell - k)$ is even. The successive coefficients which arise (for given γ and q) may usefully be gathered together in a lumped form and written as[11]

$$\bar{C}_m^{q,k} = \sum_{\ell} Q_\ell^{q,k} \bar{C}_{\ell m} , \qquad \bar{S}_m^{q,k} = \sum_{\ell} Q_\ell^{q,k} \bar{S}_{\ell m} , \tag{6}$$

where ℓ increases in steps of 2 from its minimum permissible value ℓ_0 , and the $Q_\ell^{q,k}$ are functions of inclination that can be taken as constant for a particular satellite, and $Q_{\ell 0}^{q,k} = 1$.

The rate of change of eccentricity e caused by the (ℓ,m) harmonic near $\beta{:}\alpha$ resonance can be written[11] 089

$$\frac{de}{dt} = n\left(1 - e^2\right)^{-\frac{1}{2}}\left(\frac{R}{a}\right)^{\ell}\bar{F}_{\ell mp}G_{\ell pq}\left\{\frac{q - \frac{1}{2}(k + q)e^2}{e}\right\}\mathcal{R}\left[j^{\ell-m+1}(\bar{C}_{\ell m} - j\bar{S}_{\ell m})\exp\{j(\gamma\Phi - q\omega)\}\right], \quad \ldots\ldots(7)$$

with the same definitions as for equation (4).

As the $G_{\ell pq}$ functions[11] are of order $\dfrac{(\frac{1}{2}\ell e)^{|q|}}{(|q|)!}$, it is usually found that for orbits with eccentricity <0.1 the $(\gamma,q) = (1,0)$ terms produce the most important resonance effects on the inclination. For the eccentricity, the relative importance of the terms is largely decided by the value of $\frac{1}{e}G_{\ell pq}\left\{q - \frac{1}{2}(k + q)e^2\right\}$, which is of order $\frac{1}{2}ek$ for $q = 0$, of order $\frac{1}{2}\ell$ for $q = \pm 1$ and of order $\frac{1}{2}\ell^2 e$ for $q = \pm 2$. So for the eccentricity the strongest effects are usually caused by the $(\gamma,q) = (1,1)$ and $(1,-1)$ terms, if $\ell e < 1$.

However, these rules do not always apply and 1971-106A proves to be somewhat exceptional, because the inclination is quite close to the critical inclination (63.4°) and the variation of ω is slow, the value of $\dot{\omega}$ being about 0.5 deg/day. Consequently the $(\Phi - \omega)$, Φ, and $(\Phi + \omega)$ terms in equations (4) and (7) are difficult to separate; when all three are included in the fitting, the correlations between them tend to be high, and there is a danger that the values of the coefficients obtained will have large standard deviations. So, in analysing the three resonances, the possibility arises of dropping one of the three terms to improve the separation of the coefficients. This had to be tested on all three resonances, and proved a useful stratagem in two of them.

For each of the three resonances it is necessary to choose the time interval over which the analysis is to be made. If too long a time interval is taken, the orbital parameter (i or e) will not be appreciably affected by the resonance near the ends, and it is better to concentrate the analysis in the region where the variations are strong. The danger of taking too short an interval is that there will not be enough data points. A choice between these extremes must be made. In practice the value of $\dot{\Phi}$ is used as a guide, and a range of values of $\dot{\Phi}$ between -60 and $+60$ deg/day is regarded as the outside limit, but the time interval is reduced if an adequate number of values remain: generally it is advisable to use at least 20 orbits.

5.2 14th-order (14:1) resonance

5.2.1 Equations for 14:1 resonance

089

The most important terms in equation (4) for 14:1 resonance are those with $\gamma = 1$, because $\gamma = 2$ terms are associated with harmonics of order 28 ($m = \gamma\beta$), and should be much smaller than those of order 14. Of the terms with $\gamma = 1$, those with $q = 0, 1$ and -1 are likely to be the most important, since terms with $q = \pm 2$ have an extra e factor. With $\gamma = 1$, $m = \gamma\beta = 14$ and $k = \gamma\alpha - q = 1 - q$, and concentrating on terms with $(\gamma, q) = (1,0)$, $(1,1)$ and $(1,-1)$, the affixes (q,k) in equations (6) are $(0,1)$, $(1,0)$ and $(-1,2)$. Writing only the three terms with $(\gamma,q) = (1,0)$, $(1,1)$ and $(1,-1)$ explicitly and taking $\left(1 - e^2\right)^{-\frac{1}{2}} = 1$, the theoretical variation of inclination given by equation (4) may be written for 14:1 resonance[11-14] as

$$\begin{aligned}\frac{di}{dt} = \frac{n}{\sin i}\left(\frac{R}{a}\right)^{14}\Bigg[&\frac{R}{a}(14 - \cos i)\bar{F}_{15,14,7}\left\{\bar{S}^{0,1}_{14}\sin\Phi + \bar{C}^{0,1}_{14}\cos\Phi\right\}\\
&+ \frac{15e}{2}(14)\bar{F}_{14,14,7}\left\{\bar{C}^{1,0}_{14}\sin(\Phi - \omega) - \bar{S}^{1,0}_{14}\cos(\Phi - \omega)\right\}\\
&+ \frac{11e}{2}(14 - 2\cos i)\bar{F}_{14,14,6}\left\{\bar{C}^{-1,2}_{14}\sin(\Phi + \omega) - \bar{S}^{-1,2}_{14}\cos(\Phi + \omega)\right\}\\
&+ \text{terms in}\left\{\frac{(\frac{1}{2}\ell e)^{|q|}}{(|q|)!}\,\begin{matrix}\cos\\ \sin\end{matrix}(\gamma\Phi - q\omega)\right\}\Bigg] \;. \end{aligned} \tag{8}$$

The three pairs of lumped coefficients $\bar{C}^{q,k}_m$ and $\bar{S}^{q,k}_m$ appearing in equation (8) may be written in terms of the individual geopotential coefficients $\left(\bar{C}_{\ell m}, \bar{S}_{\ell m}\right)$ as indicated in equations (6). Explicitly, with the $Q^{q,k}_\ell$ expressed in terms of the $\bar{F}$ functions, the $\bar{C}^{q,k}_m$ are[14]

$$\bar{C}^{0,1}_{14} = \bar{C}_{15,14} - \frac{\bar{F}_{17,14,8}}{\bar{F}_{15,14,7}}\left(\frac{R}{a}\right)^2\bar{C}_{17,14} + \frac{\bar{F}_{19,14,9}}{\bar{F}_{15,14,7}}\left(\frac{R}{a}\right)^4\bar{C}_{19,14} - \ldots\ldots \tag{9}$$

$$\bar{C}^{1,0}_{14} = \bar{C}_{14,14} - \frac{17\bar{F}_{16,14,8}}{15\bar{F}_{14,14,7}}\left(\frac{R}{a}\right)^2\bar{C}_{16,14} + \frac{19\bar{F}_{18,14,9}}{15\bar{F}_{14,14,7}}\left(\frac{R}{a}\right)^4\bar{C}_{18,14} - \ldots\ldots \tag{10}$$

$$\bar{C}^{-1,2}_{14} = \bar{C}_{14,14} - \frac{13\bar{F}_{16,14,7}}{11\bar{F}_{14,14,6}}\left(\frac{R}{a}\right)^2\bar{C}_{16,14} + \frac{15\bar{F}_{18,14,8}}{11\bar{F}_{14,14,6}}\left(\frac{R}{a}\right)^4\bar{C}_{18,14} - \ldots\ldots \tag{11}$$

and similarly for S, on replacing C by S throughout. The resonance angle Φ is given by equation (5) with $\alpha = 1$ and $\beta = 14$.

The most important terms in equation (7), which gives the rate of change of eccentricity, are those with $(\gamma,q) = (1,1)$ and $(1,-1)$, but for consistency with equation (8) the $(\gamma,q) = (1,0)$ terms are also given explicitly. The theoretical equation for eccentricity given by equation (7) may therefore be written for 14:1 resonance as[14]

$$
\begin{aligned}
\frac{de}{dt} = \frac{n}{2}\left(\frac{R}{a}\right)^{14} \Bigg[\Bigg[& e\left(\frac{R}{a}\right)\bar{F}_{15,14,7}\left(\bar{S}^{0,1}_{14}\sin\Phi + \bar{C}^{0,1}_{14}\cos\Phi\right) \\
& - 15\bar{F}_{14,14,7}\left\{\bar{C}^{1,0}_{14}\sin(\Phi-\omega) - \bar{S}^{1,0}_{14}\cos(\Phi-\omega)\right\} \\
& + 11\bar{F}_{14,14,6}\left\{\bar{C}^{-1,2}_{14}\sin(\Phi+\omega) - \bar{S}^{-1,2}_{14}\cos(\Phi+\omega)\right\} \\
& + \text{terms in}\left[\frac{(\tfrac{1}{2}\ell)^{|q|}e^{|q|-1}}{(|q|)!}\left\{q - \tfrac{1}{2}(k+q)e^2\right\}\begin{matrix}\cos\\ \sin\end{matrix}(\gamma\Phi - q\omega)\right]\Bigg]\Bigg] , \qquad (12)
\end{aligned}
$$

where the $\bar{C}^{q,k}_{14}$ and $\bar{S}^{q,k}_{14}$ are given by equations (9) to (11).

5.2.2 <u>Analysis of inclination, i</u>

Cosmos 462 passed through exact 14th-order resonance at MJD 41659 (1972 December 8). The effect of this resonance on the inclination has been analysed over a period of about two months either side of exact resonance, using the THROE computer program developed by Gooding[15,11], which fits the values of i with equation (4) in integrated form. During this time there were 27 values of inclination available for analysis, 10 values from the PROP orbits in Table 2 and 17 values from orbits supplied by the US Navy. All values of inclination were cleared of lunisolar and zonal harmonic perturbations using the computer program PROD[16] with one-day integration steps; for the orbits of Table 2, the $J_{2,2}$ perturbations were also removed. The US Navy values were initially given standard deviations of 0.003° and the PROP values were given their quoted standard deviations from Table 2. Four of the PROP values had their standard deviations increased to 0.0005° to allow for the neglected effect of Earth tides; one of the US Navy values was discarded because it was inaccurate and another, that at MJD 41612, had its sd increased by a factor of two.

The remaining 26 values of inclination were fitted with equation (8) using THROE, *ie* with $(\gamma,q) = (1,0)$, $(1,1)$ and $(1,-1)$. The coefficients $\left(\bar{C},\bar{S}\right)^{q,k}_{14}$ in
089 equation (8) were undetermined in this fitting, *ie* the standard deviations are of the same order as the values of the coefficients. This was to be expected

because of the correlations mentioned earlier (section 5.1) and because there were only 26 values being fitted, scarcely enough to allow a good determination of the seven coefficients (the six harmonic coefficients and the initial value of inclination).

So the values were then fitted with $(\gamma,q) = (1,0)$ only. The values of lumped harmonics obtained were

$$10^9\bar{C}_{14}^{0,1} = 62 \pm 9 , \qquad 10^9\bar{S}_{14}^{0,1} = 1 \pm 19 , \tag{13}$$

with $\varepsilon = 1.66$ (ε is as defined in section 3). A further run, with $(\gamma,q) = (1,0)$ and $(2,0)$, offered no advantage: the $(2,0)$ coefficients were undetermined and ε increased slightly. The values of the coefficients in equation (13) are satisfactory in that they provide an acceptable fitting, but they include the effects of the neglected $(1,1)$ and $(1,-1)$ terms. Values of individual 14th-order coefficients recently obtained[14] indicated that the values of $\bar{C}_{14}^{0,1}$ and $\bar{S}_{14}^{0,1}$ for 1971-106A should be approximately 9×10^{9} and -25×10^{-9}. These values are of the same order as those in equation (13) but differ sufficiently to suggest that the absorption of the $(1,1)$ and $(1,-1)$ terms does affect the values obtained.

Next the variation of inclination given by using the values $10^9\bar{C}_{14}^{0,1} = 9$ and $10^9\bar{S}_{14}^{0,1} = -25$ was calculated using THROE. It was found that the variation in inclination was extremely small, never more than $\pm 0.0008^{\circ}$. The $(1,0)$ terms were therefore discarded and the values of inclination fitted with $(\gamma,q) = (1,1)$ and $(1,-1)$. The results were fairly satisfactory, with $\varepsilon = 1.5$ and standard deviations about $\frac{1}{3}$ of the values of the coefficients.

The next point to be considered was the possibility that $(\gamma,q) = (1,2)$ and $(1,-2)$ terms might have an appreciable effect. Values of $\left(\bar{C},\bar{S}\right)_{14}^{2,-1}$ and $\left(\bar{C},\bar{S}\right)_{14}^{-2,3}$ were calculated using the values of individual 14th-order coefficients from Ref 14, and the variation of inclination due to the $(\gamma,q) = (1,2)$ and $(1,-2)$ terms was calculated using THROE. These terms produced an appreciable change in inclination at resonance, about 0.0015°. The raw values of inclination were therefore modified by subtracting the effect of the $(1,2)$ and $(1,-2)$ terms as given by this calculation and a new fitting of $(\gamma,q) = (1,1)$ and $(1,-1)$ terms was made.

The values obtained were

$$\left.\begin{aligned} 10^9\bar{C}_{14}^{1,0} &= -399 \pm 218 , & 10^9\bar{S}_{14}^{1,0} &= 394 \pm 158 \\ 10^9\bar{C}_{14}^{-1,2} &= 101 \pm 97 , & 10^9\bar{S}_{14}^{-1,2} &= 412 \pm 152 \end{aligned}\right\} \qquad (14)$$

with $\varepsilon = 1.48$. The fitting is quite good, the curve being shown as a full line in Fig 5.

The values (14) are not entirely satisfactory because of their large standard deviations, which stem from the strong correlations between coefficients - for example the correlation between $\bar{C}_{14}^{1,0}$ and $\bar{S}_{14}^{-1,2}$ is -0.953. So a better solution is likely to be possible from the simultaneous fit of inclination and eccentricity using the SIMRES [11] computer program. This will be discussed after the analysis of the values of eccentricity.

5.2.3 <u>Analysis of eccentricity, e</u>

The effect of the 14:1 resonance on the eccentricity of the orbit of 1971-106A has been analysed over the same period as the inclination, *ie* about two months either side of exact resonance, using the same 27 orbits. The US Navy values were given standard deviations of 0.00008 and the PROP values were given the standard deviations quoted in Table 2. Three of the PROP values of eccentricity had their standard deviations increased to 0.000008 to allow for the neglected effect of Earth tides, and the US Navy value dropped from the inclination analysis because of inaccuracy was also omitted here, for the same reason. All values of eccentricity were cleared of lunisolar and zonal harmonic perturbations using the PROD [16] computer program as with the inclination values.

After the first THROE fitting, with equation (12) but omitting $(\gamma, q) = (1,0)$ terms, it was apparent that the US Navy values of eccentricity suffered a bias relative to the PROP values. This mismatch between US Navy and PROP values of e has arisen previously [17], and was attributed to an inconsistency in restoring the odd-zonal harmonic perturbation to the US Navy values. Since the perturbation to e is of the form $K \sin\omega$, where K is a constant, the simplest procedure for correcting the bias is to subtract an expression of this form from the values of e, the value of K being chosen empirically to minimize the bias. Here the quantity $0.00015 \sin\omega$ was subtracted from each of the US Navy values of e.

The first THROE run after making this modification showed that the first PROP value of e, at MJD 41592, fitted badly and its sd was increased by a factor of $\sqrt{10}$. The resulting THROE run for $(\gamma,q) = (1,1)$, $(1,-1)$ gave $\varepsilon = 1.5$ and values of the coefficients with standard deviations not much smaller than the values. Next the effects of the terms $(\gamma,q) = (1,2)$, $(1,-2)$ were calculated using values of the individual coefficients from Ref 14. The variation in e due to these terms was appreciable, about 0.00003, so the values of e were cleared of this perturbation, and refitted with THROE. The resulting values of the coefficients were:

$$\left.\begin{aligned} 10^9\bar{C}_{14}^{1,0} &= -139 \pm 247\ , & 10^9\bar{S}_{14}^{1,0} &= 678 \pm 226 \\ 10^9\bar{C}_{14}^{-1,2} &= -733 \pm 154\ , & 10^9\bar{S}_{14}^{-1,2} &= -271 \pm 165 \end{aligned}\right\} \qquad (15)$$

with $\varepsilon = 1.50$. In this fitting the density scale height H was taken as 42 km, the value appropriate for a height $\frac{3}{2}H$ above perigee. (Values of 44 and 46 km were also tried, but were less satisfactory.) The fitting is quite good, the curve being shown as a full line in Fig 6, but the standard deviations of the values are too large to be regarded as satisfactory, again because of the high correlation between coefficients - for example the correlation between $\bar{S}_{14}^{1,0}$ and $\bar{C}_{14}^{-1,2}$ is 0.955. Therefore a simultaneous fitting with i is required and is discussed in the following section.

5.2.4 Inclination and eccentricity fitted simultaneously

The values of inclination and eccentricity fitted separately by THROE were next fitted simultaneously using the computer program SIMRES[11]. This program combines the results from a number of THROE runs and produces a single set of coefficients to fit the data. The program allows a choice of weighting, so that the contributing THROE runs can be given more or less weight according to their accuracy of fit, indicated by the value of ε.

Here the final THROE runs for i and e were combined and no weighting factor was applied because ε was 1.5 in both contributing THROE runs. The SIMRES fittings are shown in Figs 5 and 6 by broken lines and the values of the coefficients given by SIMRES are:

$$\left.\begin{aligned} 10^9\bar{C}_{14}^{1,0} &= 17 \pm 59 \,, & 10^9\bar{S}_{14}^{1,0} &= -137 \pm 35 \\ 10^9\bar{C}_{14}^{-1,2} &= -186 \pm 16 \,, & 10^9\bar{S}_{14}^{-1,2} &= 66 \pm 42 \end{aligned}\right\} . \tag{16}$$

The standard deviations of the values in (16) are considerably smaller than in (14) or (15), and the values should also be more reliable because the number of values being fitted is doubled. This conclusion is confirmed by Figs 5 and 6, which show that for both i and e the SIMRES fitting looks just as good as - or perhaps better than - the individual fittings. The values (16) differ from the corresponding values in (14) and (15) by between 0.5 and 3.2 times the sum of the standard deviations. The individual differences for each coefficient, expressed as multiples of the sum of the standard deviations, are as follows:

	$\bar{C}_{14}^{1,0}$	$\bar{S}_{14}^{1,0}$	$\bar{C}_{14}^{-1,2}$	$\bar{S}_{14}^{-1,2}$
i	1.5	2.8	2.5	1.8
e	0.5	3.1	3.2	1.6 .

From this table it might be expected that the values of $\bar{C}_{14}^{1,0}$ and $\bar{S}_{14}^{-1,2}$ would be more reliable than the other two.

In the recent evaluation of individual 14th-order harmonics in the geopotential[14], the lumped harmonic values in equation (16) were used in the solutions for harmonics of order 14 and even degree. It was found that the $\bar{C}_{14}^{1,0}$ and $\bar{S}_{14}^{-1,2}$ values in equation (16) made a useful contribution to the solution, yielding weighted residuals of 0.04 and 0.71 respectively in the five-coefficient solution quoted in Table 7 of Ref 14. The $\bar{S}_{14}^{1,0}$ and $\bar{C}_{14}^{-1,2}$ values in equation (16), however, did not fit so well and their standard deviations were increased by factors of 5 and 10 respectively: even then, the weighted residuals for these two coefficients in the five-coefficient solution quoted in Table 7 of Ref 14 are -1.17 and -1.14 respectively. This confirms the indication that the values of $\bar{C}_{14}^{1,0}$ and $\bar{S}_{14}^{-1,2}$ in equation (16) are more reliable than the other two.

5.3 29:2 resonance

089 The changes in inclination and eccentricity at 29:2 resonance are expected to be only $\frac{1}{8}$ as large as at 14:1 resonance, because the values of the $\bar{C}_{\ell m}$ are

likely to be only ¼ as large, and the resonance is faster because $\ddot{\Phi} \simeq \alpha \ddot{M}$ is twice as large. So the chances of successful analysis are poorer. However, the analysis needs to be made to assess the overall change in i at resonance.

5.3.1 Equations for 29:2 resonance

The most important terms in equation (4) for 29:2 resonance are those with $\gamma = 1$ and $q = 0$, 1 and -1. The $\gamma = 2$ terms are associated with harmonics of order 58 ($m = \gamma\beta$), which should be much smaller than those of order 29; and terms with $q = \pm 2$ have an extra e factor.

For the 29:2 resonance with $\gamma = 1$, $m = \gamma\beta = 29$ and $k = \gamma\alpha - q = 2 - q$, so that the affixes (q,k) in equation (6) are (0,2), (1,1) and (−1,3) when $q = 0$, 1 and −1 respectively. Writing only the three terms with $(\gamma,q) = (1,0)$, (1,1) and (1,−1) explicitly, the theoretical variation of inclination given by equation (4) may be written for 29:2 resonance[13,18] as

$$\frac{di}{dt} = \frac{n}{\sin i}\left(\frac{R}{a}\right)^{29}\Bigg[\frac{R}{a}(29 - 2\cos i)\bar{F}_{30,29,14}\left\{\bar{S}_{29}^{0,2}\sin\Phi + \bar{C}_{29}^{0,2}\cos\Phi\right\}$$
$$+ 16e(29 - \cos i)\bar{F}_{29,29,14}\left\{\bar{C}_{29}^{1,1}\sin(\Phi - \omega) - \bar{S}_{29}^{1,1}\cos(\Phi - \omega)\right\}$$
$$+ 12e(29 - 3\cos i)\bar{F}_{29,29,13}\left\{\bar{C}_{29}^{-1,3}\sin(\Phi + \omega) - \bar{S}_{29}^{-1,3}\cos(\Phi + \omega)\right\}$$
$$+ \text{terms in}\left\{\frac{(\tfrac{1}{2}\ell e)^{|q|}}{(|q|)!}\begin{matrix}\cos\\ \sin\end{matrix}(\gamma\Phi - q\omega)\right\}\Bigg] \quad . \tag{17}$$

The three pairs of lumped coefficients $\bar{C}_m^{q,k}$ and $\bar{S}_m^{q,k}$ appearing in equation (17) may be written in terms of the individual geopotential coefficients $\left(\bar{C}_{\ell m}, \bar{S}_{\ell m}\right)$ as indicated in equations (6). Explicitly, with the $Q_\ell^{q,k}$ expressed in terms of the $\bar{F}$ functions, the $\bar{C}_m^{q,k}$ are[18]

$$\bar{C}_{29}^{0,2} = \bar{C}_{30,29} - \frac{\bar{F}_{32,29,15}}{\bar{F}_{30,29,14}}\left(\frac{R}{a}\right)^2\bar{C}_{32,29} + \frac{\bar{F}_{34,29,16}}{\bar{F}_{30,29,14}}\left(\frac{R}{a}\right)^4\bar{C}_{34,29} - \ldots\ldots , \tag{18}$$

$$\bar{C}_{29}^{1,1} = \bar{C}_{29,29} - \frac{17\bar{F}_{31,29,15}}{16\bar{F}_{29,29,14}}\left(\frac{R}{a}\right)^2\bar{C}_{31,29} + \frac{18\bar{F}_{33,29,16}}{16\bar{F}_{29,29,14}}\left(\frac{R}{a}\right)^4\bar{C}_{33,29} - \ldots\ldots , \tag{19}$$

089

and

$$\bar{C}_{29}^{-1,3} = \bar{C}_{29,29} - \frac{13\bar{F}_{31,29,14}}{12\bar{F}_{29,29,13}}\left(\frac{R}{a}\right)^{2}\bar{C}_{31,29} + \frac{14\bar{F}_{33,29,15}}{12\bar{F}_{29,29,13}}\left(\frac{R}{a}\right)^{4}\bar{C}_{33,29} - \ldots\ldots , \quad (20)$$

and similarly for S, on replacing C by S throughout. The resonance angle Φ is given by equation (5) with $\alpha = 2$ and $\beta = 29$.

For the 29:2 resonance, the theoretical variation of eccentricity given by equation (7) may be written in terms of the same $\left(\bar{C}_m^{q,k}, \bar{S}_m^{q,k}\right)$ as[18]

$$\begin{aligned}\frac{de}{dt} = n\left(\frac{R}{a}\right)^{29}\Bigg[\!\!\Bigg[& - e\left(\frac{R}{a}\right)\bar{F}_{30,29,14}\left(\bar{S}_{29}^{0,2}\sin\Phi + \bar{C}_{29}^{0,2}\cos\Phi\right) \\ & - 16\bar{F}_{29,29,14}\left\{\bar{C}_{29}^{1,1}\sin(\Phi - \omega) - \bar{S}_{29}^{1,1}\cos(\Phi - \omega)\right\} \\ & + 12\bar{F}_{29,29,13}\left\{\bar{C}_{29}^{-1,3}\sin(\Phi + \omega) - \bar{S}_{29}^{-1,3}\cos(\Phi + \omega)\right\} \\ & + \text{terms in}\left[\frac{(\tfrac{1}{2}\ell)^{|q|}e^{|q|-1}}{(|q|)!}\left\{q - \tfrac{1}{2}(k+q)e^{2}\right\}\begin{matrix}\cos\\ \sin\end{matrix}(\gamma\Phi - q\omega)\right]\Bigg]\!\!\Bigg] . \quad (21)\end{aligned}$$

Three terms are given explicitly in equation (21), those with $(\gamma,q) = (1,0)$, $(1,1)$ and $(1,-1)$. The main terms are expected to be those with $(\gamma,q) = (1,1)$ and $(1,-1)$ but the $(\gamma,q) = (1,0)$ term is also given explicitly for consistency with equation (17).

5.3.2 Analysis of inclination, i

The inclination of Cosmos 462 was analysed at the time of 29:2 resonance, using 21 values of inclination, seven values being from the PROP orbits in Table 2 and 14 values from orbits supplied by the US Navy. The analysis extended to nearly two months either side of exact 29:2 resonance, which occurred at MJD 42012 (1973 November 26). All values of inclination were cleared of luni-solar and zonal harmonic perturbations using the PROD[16] program with one-day integration steps and, for the seven values from Table 2, the J_{22} perturbation. The US Navy values were given standard deviations of 0.003° and the PROP values were given their quoted standard deviations in Table 2.

089 The 21 values of inclination were then fitted with equation (17) using THROE, *ie* with $(\gamma,q) = (1,0)$, $(1,1)$ and $(1,-1)$. All the $\left(\bar{C},\bar{S}\right)_{29}^{q,k}$ coefficients

in equation (17) were undetermined in this fitting, but the fit did reveal that the US Navy values were all too large: discrepancies of this kind have been found previously[17,19,20] and are due to differences in definition in the US Navy orbits. The difficulty is avoided by making a (constant) empirical change in the US Navy values and here they were all reduced by 0.004°. The standard deviations on one PROP value of inclination, at MJD 42018, and one US Navy, at MJD 42060, were increased by a factor of two. The program was then re-run, but with similar results - all seven coefficients were undetermined, as was expected because of the correlations mentioned earlier (see section 5.1) and also because there were only 21 values being fitted.

The values were then fitted with $(\gamma,q) = (1,0)$ only, because at this resonance $e = 0.065$ and therefore the (1,1) and (1,-1) terms should not have so much effect. The values obtained were

$$10^9 \bar{C}_{29}^{0,2} = -90 \pm 74 \ , \qquad 10^9 \bar{S}_{29}^{0,2} = -127 \pm 39 \ , \tag{22}$$

with $\varepsilon = 0.689$. These values were obtained after the M_2 values on the orbits had been changed (see section 5.3.3). *The fitted curve is shown as a full line* in Fig 7. The values in equation (22) should be useful in the future in determining the individual coefficients of 29th order and even degree.

Even though the numerical values of the lumped harmonics were not particularly accurate, the fitting is useful in showing that there was an overall decrease of 0.002° in passing through 29:2 resonance and in providing end points for the analysis of atmospheric rotation (see section 6).

5.3.3 Analysis of eccentricity, e

The effect of the 29:2 resonance on the eccentricity was analysed using values of e from the same 21 orbits. All values of e were cleared of lunisolar and zonal harmonic perturbations using PROD[16]. The PROP values were given the standard deviations quoted in Table 2 and the US Navy values were given standard deviations of 0.00008. The density scale height was taken as 42 km.

After the first THROE fitting with equation (21), *ie* with $(\gamma,q) = (1,0)$, (1,1) and (1,-1), it was again apparent that the US Navy values of e suffered a bias relative to the PROP values. This bias was corrected as previously (see section 5.2.3) by subtracting an expression of the form $K \sin \omega$, where K is a constant chosen empirically to minimize the bias and taken here as 0.00045. 089
The subsequent THROE fitting with $(\gamma,q) = (1,0)$, (1,1) and (1,-1) yielded

undetermined values of the coefficients and they also had high correlations: it was obviously not possible to determine seven coefficients from 21 values.

In the course of the fitting of e, a source of error in the technique for using the THROE program became apparent. The correction of eccentricity to allow for the effects of atmospheric drag between one orbit and the next is calculated in THROE using the value of M_2 for the first of the two orbits, which is assumed to apply over the time interval between them. However, it is not correct to assume that the value of M_2 for the first orbit remains valid over the time interval between the two orbits, often seven days: for the PROP orbits the value of M_2 usually applies over about three days either side of epoch, and for the US Navy orbits for approximately five days before epoch. So the technique hitherto used was modified, and the value of M_2 at the nth epoch was taken as $\left\{(M_1)_{n+1} - (M_1)_n\right\}/2\left(t_{n+1} - t_n\right)$. This ensures that the integrated effect of air drag between epoch t_n and epoch t_{n+1} is correctly represented. This correction had an important effect in the eccentricity runs, but no significant effect for inclination, where the atmospheric corrections are very small; however, the values of M_2 were changed for i, for consistency between the fittings.

After changing the values of M_2, the values of e to be fitted, when adjusted for the effects of atmospheric drag by THROE, showed very little variation, all the values being within 0.00015 of the value 0.06900. So the chances of obtaining good lumped values of 29th-order harmonics were unpromising. Fitting with $(\gamma,q) = (1,1)$ and $(1,-1)$ gave quite undetermined values, so it was necessary to fit with $(\gamma,q) = (1,1)$ only, or $(\gamma,q) = (1,-1)$ only. These alternative fittings were very similar with $\varepsilon = 1.33$ and 1.30 respectively, but the latter seems marginally preferable because it fits the PROP values of eccentricity better. The $(\gamma,q) = (1,-1)$ fitting is shown in Fig 8.

The values obtained for the coefficients in this $(1,-1)$ fitting are $(907 \pm 325) \times 10^{-9}$ and $(-463 \pm 163) \times 10^{-9}$: these are nominally values of $\bar{C}_{29}^{-1,3}$ and $\bar{S}_{29}^{-1,3}$ respectively, but they include the effects of $\bar{C}_{29}^{1,1}$ and $\bar{S}_{29}^{1,1}$. However the results, even if the interference from $\bar{C}_{29}^{1,1}$ and $\bar{S}_{29}^{1,1}$ is slight, are not accurate enough to give numerical values useful in determining individual 29th-order coefficients. In other words, the variation in eccentricity over the region of 29:2 resonance is too small to yield good values of lumped coefficients because the orbit of 1971-106A is strongly affected by drag and the effect of
089 resonance does not last long enough for an appreciable change in e to build up.

Since the change in e is not large enough to give values of lumped coefficients, there was no purpose in making a SIMRES fitting of i and e together.

5.4 15th-order (15:1) resonance

5.4.1 Equations for 15:1 resonance

As for the two preceding resonances, the most important terms in equation (4) for 15:1 resonance are likely to be those with $\gamma = 1$, because $\gamma = 2$ terms are associated with harmonics of order 30 ($m = \gamma\beta$), and should be considerably smaller than those of order 15. Again the most important terms with $\gamma = 1$ are those with $q = 0, 1$ and -1, since $q = 2$ terms have an extra e factor. Therefore, with $\gamma = 1$, $m = 15$ and $k = \gamma\alpha - q = 1 - q$, and concentrating on terms with $(\gamma, q) = (1,0)$, $(1,1)$ and $(1,-1)$, the affixes (q,k) in equations (6) are $(0,1)$, $(1,0)$ and $(-1,2)$. So, writing only the three terms with $(\gamma,q) = (1,0)$, $(1,1)$ and $(1,-1)$ explicitly, equation (4) giving the theoretical variation of inclination may be written for 15:1 resonance[11-13] as

$$\frac{di}{dt} = \frac{n}{\sin i}\left(\frac{R}{a}\right)^{15}\Bigg[(15 - \cos i)\bar{F}_{15,15,7}\left\{\bar{C}_{15}^{0,1}\sin\Phi - \bar{S}_{15}^{0,1}\cos\Phi\right\}$$

$$+ \frac{17e}{2}(15)\left(\frac{R}{a}\right)\bar{F}_{16,15,8}\left\{\bar{S}_{15}^{1,0}\sin(\Phi - \omega) + \bar{C}_{15}^{1,0}\cos(\Phi - \omega)\right\}$$

$$+ \frac{13e}{2}(15 - 2\cos i)\left(\frac{R}{a}\right)\bar{F}_{16,15,7}\left\{\bar{S}_{15}^{-1,2}\sin(\Phi + \omega) + \bar{C}_{15}^{-1,2}\cos(\Phi + \omega)\right\}$$

$$+ \text{terms in}\left\{\frac{(\tfrac{1}{2}\ell e)^{|q|}}{(|q|)!}\begin{matrix}\cos\\ \sin\end{matrix}\left(\gamma\Phi - q\omega\right)\right\}\Bigg] \quad . \tag{23}$$

The three pairs of lumped coefficients $\bar{C}_m^{q,k}$ and $\bar{S}_m^{q,k}$ appearing in equation (23) may be written in terms of the individual geopotential coefficients $\left(\bar{C}_{\ell m}, \bar{S}_{\ell m}\right)$ as indicated in equation (6). Explicitly, with the $Q_\ell^{q,k}$ expressed in terms of the $\bar{F}$ functions, the $\bar{C}_m^{q,k}$ are[11]

$$\bar{C}_{15}^{0,1} = \bar{C}_{15,15} - \frac{\bar{F}_{17,15,8}}{\bar{F}_{15,15,7}}\left(\frac{R}{a}\right)^2\bar{C}_{17,15} + \frac{\bar{F}_{19,15,9}}{\bar{F}_{15,15,7}}\left(\frac{R}{a}\right)^4\bar{C}_{19,15} - \ldots\ldots \tag{24}$$

$$\bar{C}_{15}^{1,0} = \bar{C}_{16,15} - \frac{19\bar{F}_{18,15,9}}{17\bar{F}_{16,15,8}}\left(\frac{R}{a}\right)^2\bar{C}_{18,15} + \frac{21\bar{F}_{20,15,10}}{17\bar{F}_{16,15,8}}\left(\frac{R}{a}\right)^4\bar{C}_{20,15} - \cdots\cdots \tag{25}$$

$$\bar{C}_{15}^{-1,2} = \bar{C}_{16,15} - \frac{15\bar{F}_{18,15,8}}{13\bar{F}_{16,15,7}}\left(\frac{R}{a}\right)^2\bar{C}_{18,15} + \frac{17\bar{F}_{20,15,9}}{13\bar{F}_{16,15,7}}\left(\frac{R}{a}\right)^4\bar{C}_{20,15} - \cdots\cdots \tag{26}$$

and similarly for S, on replacing C by S throughout. The resonance angle Φ is given by equation (5) with $\alpha = 1$ and $\beta = 15$.

For the 15:1 resonance, the theoretical variation of eccentricity given by equation (7) may be written in terms of the same $\left(\bar{C}_m^{q,k}, \bar{S}_m^{q,k}\right)$ as[11,12]

$$\begin{aligned}
\frac{de}{dt} = \frac{n}{2}\left(\frac{R}{a}\right)^{15}\Bigg[\!\!\Bigg[& e\bar{F}_{15,15,7}\left(\bar{C}_{15}^{0,1}\sin\Phi - \bar{S}_{15}^{0,1}\cos\Phi\right) \\
& - 17\left(\frac{R}{a}\right)\bar{F}_{16,15,8}\left\{\bar{S}_{15}^{1,0}\sin(\Phi-\omega) + \bar{C}_{15}^{1,0}\cos(\Phi-\omega)\right\} \\
& + 13\left(\frac{R}{a}\right)\bar{F}_{16,15,7}\left\{\bar{S}_{15}^{-1,2}\sin(\Phi+\omega) + \bar{C}_{15}^{-1,2}\cos(\Phi+\omega)\right\} \\
& + \text{terms in}\left[\frac{(\frac{1}{2}\ell)^{|q|}e^{|q|-1}}{(|q|)!}\left\{q - \tfrac{1}{2}(k+q)e^2\right\}\begin{matrix}\cos\\ \sin\end{matrix}(\gamma\Phi - q\omega)\right]\Bigg]\!\!\Bigg] .
\end{aligned} \tag{27}$$

Three terms are given explicitly in equation (27), those with $(\gamma,q) = (1,0)$, $(1,1)$ and $(1,-1)$. The main terms, as with the previous two resonances, are expected to be those with $(\gamma,q) = (1,1)$ and $(1,-1)$, but the $(\gamma,q) = (1,0)$ term is given for consistency with equation (23).

5.4.2 Analysis of inclination, i

At the time of 15th-order resonance, nine PROP orbits from Table 2 and 13 US Navy orbits were available for analysis. The analysis covers a period of approximately two months before and one month after the date of exact 15:1 resonance, MJD 42302 (1974 September 12). All values of inclination were cleared of lunisolar and zonal harmonic perturbations using the PROD[16] program with one-day integration steps; and the nine values from Table 2 were cleared of the J_{22}
089 perturbation. The US Navy values were given standard deviations of 0.003° and the PROP values were given their quoted standard deviations in Table 2.

The 22 values of inclination were fitted with equation (23) using THROE, *ie* with $(\gamma,q) = (1,0)$, $(1,1)$ and $(1,-1)$. The coefficients $(\bar{C},\bar{S})_{15}^{q,k}$ in equation (23) were undetermined in this fitting, so the values were then fitted with just $(\gamma,q) = (1,0)$. For this fitting the US Navy value at MJD 42333 was dropped because it was inaccurate and the M_2 values on the orbits were changed as for the 29:2 resonance (see section 5.3.3). The values obtained were

$$10^9\bar{C}_{15}^{0,1} = -36 \pm 21\,, \qquad 10^9\bar{S}_{15}^{0,1} = 9 \pm 17\,, \tag{28}$$

with $\varepsilon = 1.102$. The fitted curve is shown as a full line in Fig 9. These values of $(\bar{C},\bar{S})_{15}^{0,1}$ are quite small and consequently not well determined. Previous evaluations of 15th-order coefficients[21] indicate that at inclinations near 65° the values of both $\bar{C}_{15}^{0,1}$ and $\bar{S}_{15}^{0,1}$ are near zero, and of order $(0 \pm 20) \times 10^{-9}$; the variation of $\bar{C}_{15}^{0,1}$ and $\bar{S}_{15}^{0,1}$ near 65° is not very well defined in Ref 21 because the only value available near 65° - Cosmos 387 at 62.9° - may not be entirely reliable, as the data on which it is based are very limited.

As the $(\bar{C},\bar{S})_{15}^{0,1}$ coefficients are small *for 1971-106A, it was worth fitting* the inclination values with $(\gamma,q) = (1,1)$ and $(1,-1)$. The values obtained were

$$\left.\begin{aligned} 10^9\bar{C}_{15}^{1,0} &= 29 \pm 83\,, & 10^9\bar{S}_{15}^{1,0} &= 196 \pm 142 \\ 10^9\bar{C}_{15}^{-1,2} &= 116 \pm 124\,, & 10^9\bar{S}_{15}^{-1,2} &= 145 \pm 97 \end{aligned}\right\} \tag{29}$$

with $\varepsilon = 1.096$. These results were then used with the results for eccentricity in a SIMRES fitting (section 5.4.4).

5.4.3 Analysis of eccentricity, e

The same 21 orbits used in analysing the inclination were analysed to determine the effect of 15:1 resonance on the eccentricity: the US Navy value at MJD 42333 was dropped again because it was inaccurate. All the 21 values of e were cleared of lunisolar and zonal harmonic perturbations using PROD[16]. The PROP values were given the standard deviations quoted in Table 2 and the US Navy values were given standard deviations of 0.00008. The density scale height was taken as 35.5 km.

After the first THROE fitting with equation (27) it was again apparent that the US Navy values suffered a bias relative to the PROP values (see section 5.2.3). To overcome this bias, the quantity 0.0002 sin ω was subtracted from each US Navy value of eccentricity. In order to obtain the right adjustment for the effects of atmospheric drag by THROE, the values of M_2 were changed using the technique described in section 5.3.3.

After the first fitting with THROE, with $(\gamma,q) = (1,0)$, $(1,1)$ and $(1,-1)$, it was apparent that seven coefficients could not be determined from 21 values of eccentricity. As the $(1,0)$ terms have very little effect on eccentricity, the values were next fitted with $(\gamma,q) = (1,1)$ and $(1,-1)$. The values of the lumped coefficients obtained were

$$\left.\begin{array}{llll} 10^9\bar{C}_{15}^{1,0} = 124 \pm 64 \,, & 10^9\bar{S}_{15}^{1,0} = 28 \pm 104 \\ 10^9\bar{C}_{15}^{-1,2} = -154 \pm 89 \,, & 10^9\bar{S}_{15}^{-1,2} = -6 \pm 54 \end{array}\right\} \qquad (30)$$

with $\varepsilon = 1.469$. The fitted curve is shown as a full line in Fig 10. The values of all the coefficients in equation (30) agree with those from equation (29) to within 1.3 times the sum of their standard deviations. So the prospect of achieving a better fit with SIMRES is good.

5.4.4 Inclination and eccentricity fitted simultaneously

The values of inclination and eccentricity fitted separately by THROE with $(\gamma,q) = (1,1)$ and $(1,-1)$ were next fitted simultaneously using the computer program SIMRES[11]. As explained in section 5.2.4, this program allows a choice of weighting. In the first fitting, i and e were given equal weight and in the second e was degraded by a factor equal to the ratio of the final values of ε on the THROE fittings, namely 1.340 (= 1.469/1.096). The second fitting is the more logical, and gave lower standard deviations for all four lumped coefficients; so it was preferred. The fittings are shown in Figs 9 and 10 by broken lines, and it is very satisfactory that these are just as good as the separate fittings (unbroken lines). The values of the lumped coefficients given by SIMRES are

$$\left.\begin{array}{llll} 10^9\bar{C}_{15}^{1,0} = 51 \pm 24 \,, & 10^9\bar{S}_{15}^{1,0} = -55 \pm 7 \\ 10^9\bar{C}_{15}^{-1,2} = -67 \pm 10 \,, & 10^9\bar{S}_{15}^{-1,2} = -19 \pm 24 \end{array}\right\} . \qquad (31)$$

)89

It can be seen that the standard deviations here are much lower than those in equations (29) and (30), so the combined fitting is well worthwhile. The values in equations (31) differ from the corresponding values in equations (29) by less than 1.7 times the sum of the standard deviations and from the corresponding values in equations (30) by less than 0.9 times the sum of the standard deviations. The individual differences for each coefficient expressed as multiples of the sum of the standard deviations are as follows:

	$\bar{C}_{15}^{1,0}$	$\bar{S}_{15}^{1,0}$	$\bar{C}_{15}^{-1,2}$	$\bar{S}_{15}^{-1,2}$
i	0.2	1.7	1.4	1.4
e	0.8	0.7	0.9	0.2 .

The lumped coefficients in equations (31) should be useful in a future determination of the individual coefficients of the 15th-order and even degree. In a previous determination[22] there were no reliable values for inclinations near 65°.

6 ATMOSPHERIC ROTATION

6.1 Introduction

The upper atmosphere is rotating at approximately the same rate as the Earth: therefore the aerodynamic force acting on a satellite has a component perpendicular to the orbit, and this has the effect of reducing the inclination, i , of the orbit during the course of the satellite's life. For a high-drag satellite, atmospheric rotation is the most important force perturbing i ; so if the change in i is accurately measured, and other perturbations are removed, the rotation rate of the upper atmosphere in the region near the satellite's perigee can be determined, *ie* the zonal (west-to-east) wind speed near perigee can be evaluated.

The perturbations to be removed are caused by (1) lunisolar gravitational attraction, (2) zonal harmonics in the geopotential, (3) the J_{22} tesseral harmonic, (4) any change in i due to resonance and (5) the change in inclination due to meridional winds. The values of inclination are cleared of the effects of (1) and (2) using the computer program PROD[16] with one-day integration steps. The effect of perturbation (3) is removed by calculation of its numerical value for each PROP orbit. The resonances have already been analysed in section 5, and the effects of meridional winds and other perturbations are discussed in section 6.3.

089

6.2 Theory

The change Δi in the inclination of a satellite's orbit, due to atmospheric rotation, is given in terms of the change ΔT_d in the satellite's orbital period, due to drag, by the equation[23]

$$\left[6\sqrt{F}\left\{1 + 2e\frac{I_1}{I_0} + \frac{3}{4}e^2\left(1+\frac{I_2}{I_0}\right) + c\left(\frac{I_2}{I_0} + 2e\frac{I_3}{I_0}\right)\cos 2\omega\right\}\right]\frac{\Delta i}{\Delta T_d}$$

$$= \Lambda \sin i\left[1 + \frac{I_2}{I_0}(1+c)\cos 2\omega - 2e\frac{I_1}{I_0}(1+\cos 2\omega) + \frac{1}{2}c\left(1+\frac{I_4}{I_0}\cos 4\omega\right) - ce\left\{(1+\cos 2\omega)\frac{I_1}{I_0} + \frac{I_3}{I_0}\cos 2\omega\right\} + e^2\left\{\left(\frac{3}{4}+\frac{11}{8}\cos 2\omega\right) + \frac{1}{4}(1-\cos 2\omega)\frac{I_2}{I_0}\right\} + O(c^3,e^3)\right] . \qquad (32)$$

In equation (32), which applies for an eccentricity of 0.2 or less, Λ is the angular velocity of the atmosphere (about the Earth's axis) in the region near perigee, divided by the Earth's angular velocity: thus Λ is strictly non-dimensional, but can conveniently be expressed in rev/day because the Earth's rotation rate is 1.0 rev/day. In equation (32) the change in orbital period ΔT_d is expressed as a fraction of a day; the term in $\cos 4\omega$, which was neglected in Ref 23, has been restored.

Other parameters in equation (32) are as follows: the I_n are the Bessel functions of the first kind and imaginary argument, of degree n and argument $z = ae/H$, where H is the atmospheric density scale height. The parameter c takes account of atmospheric oblateness and is given by $c = \left\{\varepsilon' a(1-e)\sin^2 i\right\}/2H$, where ε' is the ellipticity of the atmosphere, taken the same as that of the Earth, 0.00335. The factor F is given by $\sqrt{F} = \left\{1 - a(1-e)w\cos i\right\}/V_p$, where V_p is the satellite's velocity at perigee and w is the angular velocity of the atmosphere near perigee. Usually $\sqrt{F}$ has a value between 0.95 and 1.05. For 1971-106A, at inclination 65.7° with perigee height near 200 km, $\sqrt{F} \simeq 1 - 0.0025\Lambda$.

The change in inclination due to meridional winds is given by[24]

089 $$\frac{\Delta i}{\Delta T_d} = -\frac{\mu}{3\sqrt{F}}\cos i\left\{\frac{2}{1+\cos^2 i}\right\}^{\frac{1}{2}}\left\{\left(1-\frac{K}{4}\right)\frac{I_1}{I_0}\cos\omega - \frac{KI_3}{4I_0}\cos 3\omega + O(0.1,e)\right\}, \qquad (33)$$

where $K = \sin^2 i/(1 + \cos^2 i)$ and μ is the south-to-north atmospheric rotation rate, that is the south-to-north wind speed (m/s) divided by rw_E where r is the distance from Earth's centre (m) and w_E is the angular velocity of the Earth (72.7×10^{-6} rad/s); so $rw_E = 6580000 \times 72.7 \times 10^{-6} = 478$ m/s if perigee height is near 200 km.

6.3 Fitting of theoretical curves to the inclination

The values of orbital inclination from the 85 orbits of Table 2 and the 15 orbits of Table 4 have been cleared of the effects of lunisolar, zonal harmonic and J_{22} tesseral harmonic perturbations, and the values have been plotted as circles in Figs 11 and 12. The 15 values of Fig 12 can be regarded as superseding the last three values of Fig 11.

Perturbations in inclination due to Earth and ocean tides and solar radiation pressure have not been taken into account. The tidal perturbation in i for Geos 1, a satellite with an orbital inclination similar to 1971-106A, amounts[25] to $\pm 0.0004^\circ$. To allow for the neglect of this effect, all the standard deviations less than 0.0005° have been increased to 0.0005°. The effect of solar radiation pressure is very small: its effect on Explorer 24, a satellite in a comparable orbit but of much higher area-to-mass ratio (which was analysed by Slowey[26]), shows that the effect of solar radiation pressure on i for Cosmos 462 is likely to be of order 0.00001°.

The theoretical variation of i due to atmospheric rotation and meridional winds can be determined for a series of values of Λ and μ, using a computer program (ROTATM) based on equations (32) and (33). The theoretical variation of i was calculated for values of Λ between 0.8 and 1.4 at intervals of 0.1, with $\mu = 0$ and 0.2, every 20 days throughout the satellite's life until the last 15 days, when the variation of i was evaluated daily. The values of i in Figs 11 and 12 were then fitted with the best theoretical curves. Fig 11 divides naturally into four sections separated by the perturbations in inclination at 14:1, 29:2 and 15:1 resonances. These resonances have been analysed in section 5 and the change in inclination due to resonance is available for each resonance. At the end of each resonance period the curve for atmospheric rotation is started at the value of i given at the end of resonance in the resonance analysis (see Figs 5, 7 and 9), with atmospheric rotation perturbations restored. There is a fifth section to be fitted with a theoretical curve, for the last 15 days when the daily orbits are available (Fig 12).

The variations in i due to meridional rotation, south-to-north winds, are proportional to $\cos\omega$ (see equation (33)) and therefore the effect usually cancels out over one cycle of ω for a fixed value of μ. However, the value of μ itself varies and both theoretical studies[27-29] and experimental results[29-32] suggest that μ has an approximately sinusoidal variation during the course of 24 hours; with maximum wind towards the equator at about 02 h local time and maximum wind away from equator at about 14 h. For 1971-106A the variation in ω is slow (one cycle in 1.8 yr approximately, see Fig 3) and the local-time variations, indicated at the top of Fig 11, are much faster, one cycle every 90 days approximately. The first four sections in Fig 11 are all averaged in local time, covering about 200 days. The effect of μ will therefore tend to cancel out, and the fittings were made with the $\mu = 0$ curves. It is possible that the mean value of μ is non-zero, but the effect is generally small: on the first section, for example, the effect of $\mu = 0.05$ throughout would be to change i by 0.0005°.

So the values of inclination are fitted by choosing the best values of Λ assuming $\mu = 0$ on the first four sections. After allowance has been made for the breaks at resonance, the best fit between theory and observations for the four sections of Fig 11 was obtained with values of atmospheric rotation Λ of 1.1, 0.9, 1.0 and 1.0 respectively.

In order to assess the likely errors in these values of Λ, a realistic estimate of the likely errors in i at the beginning (i_B) and end (i_E) of each section, σ_B and σ_E, was made, and then $\Lambda\sqrt{\sigma_B^2 + \sigma_E^2}/(i_B - i_E)$ was taken as the standard deviation in Λ. For the first three sections of the curve in Fig 11 the errors σ_B and σ_E are estimated as being between 0.0005° and 0.0007°, and this gives errors in Λ of near 0.05 on all three sections. For the fourth section the error in Λ is 0.02 on the same basis. This value is so small that other errors, hitherto neglected, may become significant: there is a possible error of about 0.01 from the neglect of $O(c^3)$ terms in equation (32), and possibly errors approaching 0.01 from errors in the assumed atmospheric ellipiticity. There may also be a small error, not more than 0.02, from neglect of the effects of 31:2 resonance.

There is a possibility that the atmospheric winds depend on season, so the latitude and 'seasonal bias' of perigee are indicated below the curve in Fig 11.

In fitting the values of inclination in the last 15 days of the life, Fig 12, the effect of meridional winds should be included. The season is near equinox
089 and the perigee latitude is 54-62°N: in these conditions, the prevailing winds are[27-32] from north to south of order 100 m/s at local times from 23 h through

midnight to 05 h, with only very weak winds from 17-23 h local time. So it is appropriate in Fig 12 to take $\mu = -0.2$ up to March 30, and $\mu = 0$ thereafter. With these values of μ, the best fit is obtained with $\Lambda = 1.1$: the curve fits all the 15 values in Fig 12 to within 1.5 sd, and, taking σ_B and σ_E as slightly less than 0.001°, the sd in Λ is assessed as 0.1.

6.4 Results

Previous studies[33] of upper-atmosphere zonal winds have shown that the value of Λ varies with both height and local time. Fig 13 of Ref 33 gives three curves for the variation of Λ with height, for evening (18-24 h), morning (04-12 h) and average values of local time. A revised version of this diagram is given as Fig 2 of Ref 34.

Table 5

Values of atmospheric rotation rate, Λ, obtained from 1971-106A

Date	Height km	Local time	'Seasonal bias'	Λ
21 Jan - 2 Oct 1972	253	Av	Winter	1.1 ± 0.05
30 Jan - 30 Sep 1973	250	Av	Summer	0.9 ± 0.05
20 Jan - 14 Jul 1974	239	Av	Average	1.0 ± 0.05
24 Oct 1974 - 19 Mar 1975	218	Av	Average	1.0 ± 0.03
19 Mar - 4 Apr 1975	199	03-21 h	-	1.1 ± 0.1

The results obtained here are listed in Table 5. The values of Λ are given for each section of Fig 11 and for Fig 12, together with an estimate of the height and local time at which the values apply. The 'seasonal bias', as given by the latitude of perigee and time of year (see Fig 11), is also indicated. The height is taken as $\frac{3}{4}H$ above the average perigee height[35].

The first section of the fitted curve in Fig 11 gives a value of $\Lambda = 1.1$, and during nearly the whole of this period the perigee is experiencing 'winter' conditions. For the second section, with $\Lambda = 0.9$, the perigee is enjoying predominantly 'summer' conditions; for the third and fourth sections, where $\Lambda = 1.0$, perigee has average seasonal conditions. (Although the third section may seem to have a bias towards 'winter' the short 'summer' occurs during the time of greatest change in i.) These results suggest that Λ may be higher in winter than in summer. Such a seasonal dependence of Λ has not been detected before in the analysis of satellite orbits, but measurements at specific sites by the radar back-scatter method[31,36,37] indicate that the strongest west-to-east winds 089 usually occur in the winter, *ie* Λ is higher in the winter. The results here lend support to this conclusion.

The first four values of Λ in Table 5 (for average local time) are all below the average curve in Fig 13 of Ref 33. This decrease in the value of Λ can also be detected in other analyses of satellite orbits[38-40] between 1971 and 1976, when compared with the average curve of Ref 33, which is based mainly on results from the 1960s. So it seems possible that the average rotation rate of the upper atmosphere has decreased during the early 1970s: further evaluations of atmospheric rotation rate are needed before this tentative conclusion can be confirmed.

The value obtained for the last 15 days in orbit, $\Lambda = 1.1 \pm 0.1$ at a height of 199 km, is at a time close to equinox, but it is not averaged over all local times like the other values. The local time runs from 03 h through midnight to 21 h and there is a mild bias towards the evening hours because the decrease in inclination is then more rapid. So the value might be described as 'average with a slight bias towards evening', and indicates west-to-east winds of 25 ± 25 m/s at an average latitude of 58°N. Results for such high latitudes are unusual in satellite orbital analysis, because the effect of atmospheric rotation becomes very small as perigee approaches apex (maximum latitude) and it is not usually possible to obtain accurate values of Λ. The successful results obtained here are attributable to (a) the large change in orbital period in the last few days before decay, and (b) the frequent and accurate orbits obtained with the aid of the NORAD observations.

7 DENSITY SCALE HEIGHT

7.1 Introduction

The perigee distance, $a(1 - e)$, gradually decreases under the influence of air drag, and the decrease is proportional to the density scale height, H. So values of H can be found from the decrease in $a(1 - e)$. If the odd zonal harmonic and lunisolar perturbations are removed from $a(1 - e)$, using PROD[16], the remaining variation should show a steady decrease as a result of air drag alone. These 'corrected' values of perigee distance, Q, for the 85 orbits of Table 2 are plotted as crosses in Fig 3 of Ref 7, with a smooth curve drawn through the points. This graph has been reproduced here as Fig 13. The values of $a(1 - e)$ for the 15 daily orbits before decay (Table 4) are plotted as
089 circles in Fig 14, and after removal of perturbations are plotted as crosses with a smooth curve drawn through the values. The curve of Fig 14 can be regarded as

superseding that of Fig 13 from MJD 42492 onwards. The variation of Q, in Figs 13 and 14, shows a fairly smooth decrease due to the action of air drag.

7.2 Method

The theoretical equation for the variation of Q is[41]

$$\dot{Q} = -\frac{2H_1M_2}{3M_1e}\left\{1 - 2e + \frac{H_1}{4ae} - \frac{2\varepsilon'}{e}\sin^2 i\cos 2\omega + O\left(e^2, \frac{H}{a}, \frac{H^2}{a^2e^2}, \frac{\varepsilon'^2}{e^2}\right)\right\}, \qquad (34)$$

where H is the density scale height, H_p is the value of H at perigee, H_1 is the value of H at a height $1.5\,H_p$ above perigee, and ε' is the ellipticity of the atmosphere, taken as equal to the Earth's ellipticity, 0.00335. Equation (34) is valid for $ae/H_p > 3$.

Average values of $\dot{Q}$ were calculated over a time-interval, Δt, long enough to ensure that an accurately measurable change, ΔQ, in Q, has occurred. The values of $\Delta Q/\Delta t$ serve as values of $\dot{Q}$ in equation (34), and averaged values of M_1, M_2, e, a, i and $\cos 2\omega$ over the corresponding Δt were used to calculate values of H_1 from equation (34).

For 1971-106A, the value of ae/H_p exceeds 3 from launch until MJD 42495, and 17 values of H_1 were calculated during this time: they are plotted as circles in Fig 15, and the time over which they are averaged is indicated. The corresponding average values of height $y_1 (= y_p + 1.5\,H_p)$ are given at the top of Fig 15. The standard deviations in the values of H_1 derive from the estimated errors in the values of ΔQ arising from errors in Q. The errors due to neglected terms in (34) are smaller than the errors in ΔQ, and are ignored.

After MJD 42495, when the value of ae/H_p falls below 3, equation (34) becomes inaccurate, and the small-eccentricity form of the theory[42,43] must be used. The theoretical equation for H_1 when $ae/H_p < 3$ is $H_1 = \Delta Q/f(z)$, where $z = ae/H_1$ and

$$f(z) = \left\{\left(r_{p_1} - r_p\right)\Big/H\right\}_{\text{sph.atm.}} - \left\{\psi(z) - \psi(z_1)\right\}. \qquad (35)$$

Values of $\left(r_{p_1} - r_p\right)\Big/H$ for a spherical atmosphere are given in Fig 18 of Ref 42; and $\left\{\psi(z) - \psi(z_1)\right\}$, the oblateness correction, is given in Fig 22 of Ref 42. The values of H_1 apply at a height γH_p above perigee, where γ is given in Fig 9 of Ref 43. Seven values of H_1 were evaluated between MJD 42495 and decay, the 089 last four being daily values. For these seven values, the observed values of e must be corrected for the odd-harmonic oscillation, and this was done using PROD[16]. These seven values of H_1 are also plotted as circles in Fig 15 with their standard deviations. The sd is the estimated error in the value of ΔQ (between 1.2% and 3.8%) arising from errors in Q, together with the estimated error in reading Figs 18 and 22 of Ref 42 (between 2% and 6%). The errors due to neglected terms in equation (35) should be[42] less than 1%, and are ignored. The corresponding average values of height $y_1 (= y_p + \gamma H_p)$ are given at the top of Fig 15.

The values of H_1 plotted as crosses in Fig 15 are the values of density scale height obtained from the COSPAR International Reference Atmosphere 1972[44] for heights y_1 and the appropriate exospheric temperatures, T_∞, obtained from Ref 7.

7.3 Discussion of results

The general impression gained from studying Fig 15 is that the *CIRA 1972* values are in fairly good agreement with the values from the orbital analysis. This confirms the accepted opinion that *CIRA 1972* represents the scale height H, a very variable parameter, fairly accurately. The average difference between the observational and *CIRA 1972* values in Fig 15 is about 1%, while the rms difference is about 10%.

Three of the observational values in Fig 15 differ from the *CIRA* values by more than 5 km, those at MJD 41859-42018 (1973 June 26 - December 2), MJD 42253-42329 (1974 July 25 - October 9) and MJD 42398-42438 (1974 December 17 - 1975 January 26).

The first of these values is low compared with that given by *CIRA*, probably because the density is low over this period, relative to other years (see Fig 14 of Ref 7). The second value, which is higher than *CIRA*, is at a time when density is fairly average (see Fig 14 of Ref 7), though it is rising towards the end of the period; so no reason for this high value can be given. The third value, from 1974 December 17 to 1975 January 26, which is also higher than *CIRA*, is however explained by the above-average values of density over the whole period (see Fig 8 of Ref 7).

The results also show that it is possible to obtain accurate and consistent daily values of H at the end of the satellite's life when good orbits are available from numerous observations. These last few values are also in good
089 agreement with *CIRA 1972*.

8 CONCLUSIONS

The orbit of 1971-106A has been determined at 85 epochs during its 40-month life from 6635 observations. The accurate Hewitt camera observations were used in 24 of these orbits, in which the average sd in inclination corresponds to about 80 m in distance; while for the other 61 orbits the average sd corresponds to about 170 m in distance. The other orbital parameters show improved accuracy with the camera observations, but to a lesser degree. The residuals of the observations have been sent to the observers.

A further 2000 observations were received from NORAD covering the last 15 days of the satellite's life. With these observations, 15 daily orbits were determined. These orbits at the end of the satellite's life are more accurate and at closer intervals than has been possible in the past; the average sd in inclination corresponds to about 120 m in distance.

Analysis of the inclination and eccentricity at 14:1, 29:2 and 15:1 resonances, has yielded lumped values of the harmonic coefficients of order 14, 29 and 15. The lumped 14th-order coefficients from fitting i and e with SIMRES are given in equation (16) and have been used in a recent evaluation of the 14th-order harmonics. The analysis of the change in inclination at 29:2 resonance yielded lumped coefficients, equation (22), which should be useful in the future in determining the individual coefficients of order 29. The variation in eccentricity was too small to analyse successfully. The SIMRES fitting of inclination and eccentricity at 15th-order resonance was very satisfactory. The lumped coefficients are given in equation (31) and will be useful in a further determination of the individual coefficients of 15th order.

The variation of inclination between the resonances has been analysed to obtain four values of the average atmospheric rotation rate, Λ. The results are summarized in Table 5. Because of the very slow movement of perigee, two of the values of Λ had strong seasonal bias and the results suggest that Λ may be higher in winter than in summer. This seasonal difference has not been detected before from analysis of satellite orbits, but is in agreement with measurements at specific sites by the radar back-scatter method. The values of Λ are lower than expected, and it seems possible that the average rotation rate of the upper atmosphere was lower during the early 1970s than in the 1960s. The daily orbits over the last 15 days of the satellite's life give west-to-east winds of
25 ± 25 m/s at an average latitude of 58°N. Results for such high latitude are 089
unusual, but are possible here due to the large change in orbital period in the

last few days before decay, and the frequent and accurate orbits obtained with the aid of NORAD observations.

Values of density scale height, H_1 have been determined from analysis of the variation of perigee height. A total of 24 values was obtained during the satellite's 40-month life: eight of these were in the last 15 days of the life and the last four were daily. The values obtained show fairly good agreement with *CIRA 1972*; the average difference between the observational and *CIRA 1972* values is about 1% and the rms difference 10%. Only three observational values differ from *CIRA 1972* by more than 5 km and reasons for two of these differences have been suggested. The agreement shows that *CIRA 1972* provides a good measure of the density scale height for the years 1972-1975.

Table 2

VALUES OF THE ORBITAL PARAMETERS AT 85 EPOCHS, WITH STANDARD DEVIATIONS

	MJD	Date	a	e	i	Ω	ω	M_0	M_1	M_2	M_3	M_4	M_5	ε	N	D	a(1 - e)
1*	41337	21 Jan 1972	7374.904	0.105214	65.7435	176.133	30.84	321.45	4935.575	0.1963	0.00230	0.00052	-	0.90	45	9.1	6598.96
			1	7	4	1	1	1	1	5	7	2					
2	41362	15 Feb 1972	7364.928	0.104027	65.7451	113.068	18.77	359.27	4945.609	0.2240	0.00233	-0.00016	-	0.99	44	9.4	6598.78
			1	10	18	2	1	1	1	3	5	2					
3*	41381	5 Mar 1972	7354.598	0.102880	65.7390	64.926	9.57	101.08	4956.033	0.2939	0.00011	0.00066	-	0.76	70	7.5	6597.96
			1	8	1	<1	<1	<1	1	5	9	5					
4	41390	14 Mar 1972	7348.950	0.102185	65.7375	42.039	5.23	90.74	4961.749	0.3286	0.00294	0.00037	-	0.68	78	9.9	6598.00
			<1	9	11	1	<1	<1	<1	3	3	1					
5*	41398	22 Mar 1972	7343.143	0.101481	65.7429	21.646	1.34	207.83	4967.637	0.3788	0.00128	-		0.62	60	5.8	6597.95
			1	14	5	1	1	1	1	3	21						
6*	41404	28 Mar 1972	7338.621	0.100938	65.7451	6.318	358.43	147.53	4972.231	0.3635	-0.00331	-		0.62	43	5.7	6597.88
			2	29	10	2	1	1	2	5	29						
7	41431	24 Apr 1972	7322.282	0.099097	65.7332	297.007	345.20	347.63	4988.885	0.2602	-0.00425	-0.00013	-	0.74	61	9.1	6596.67
			1	15	15	2	1	1	1	5	7	3					
8	41462	25 May 1972	7308.221	0.097363	65.7338	216.890	329.98	68.14	5003.292	0.2162	-0.00143	-		0.53	50	7.4	6596.67
			1	15	13	1	1	1	1	2	13						
9	41471	3 Jun 1972	7304.608	0.096920	65.7310	193.543	325.54	114.57	5007.005	0.2143	0.00294	-		0.60	59	8.0	6596.65
			1	12	10	1	1	1	1	2	9						
10*	41498	30 Jun 1972	7292.025	0.095414	65.7332	123.235	312.14	120.08	5019.972	0.2124	-0.00290	-		0.47	47	5.0	6596.26
			1	12	8	1	1	1	1	5	31						
11	41507	9 Jul 1972	7288.338	0.094992	65.7319	99.715	307.66	316.58	5023.783	0.2232	-0.00222	-0.00028	-	0.81	62	8.7	6596.00
			2	18	20	2	1	1	2	6	14	4					
12	41526	28 Jul 1972	7281.857	0.094181	65.7293	49.948	298.18	74.60	5030.492	0.1576	-0.00154	-		0.49	30	4.9	6596.04
			2	12	17	1	1	1	2	9	42						
13	41534	5 Aug 1972	7279.267	0.093876	65.7284	28.948	294.23	8.38	5033.178	0.2490	0.00215	-0.00273	-	0.78	49	7.1	6595.92
			2	12	19	2	1	1	2	12	22	10					
14	41552	23 Aug 1972	7273.706	0.093184	65.7351	341.616	285.16	300.09	5038.953	0.1676	-0.00089	0.00020	0.00007	0.42	70	9.7	6595.91
			1	7	10	1	1	1	1	3	18	1	1				
15	41562	2 Sep 1972	7269.595	0.092708	65.7375	315.269	280.19	309.36	5043.228	0.2449	-0.00034	-0.00023	-	0.44	54	7.3	6595.65
			1	8	10	1	1	1	1	7	10	5					
16	41575	15 Sep 1972	7263.646	0.091958	65.7293	280.941	273.66	31.20	5049.426	0.2684	-0.00403	-0.00152	-	0.55	61	5.3	6595.70
			1	10	13	1	1	1	1	13	31	20					
17*	41592	2 Oct 1972	7255.616	0.090996	65.7293	235.906	265.10	262.13	5057.812	0.2180	-0.00119	0.00105	-0.00023	0.48	82	6.9	6595.38
			1	6	4	1	1	1	1	12	46	14	4				
18	41607	17 Oct 1972	7249.712	0.090246	65.7299	196.055	257.49	215.31	5063.994	0.2015	0.00197	0.00190	-	0.47	80	5.0	6595.45
			2	9	10	1	1	1	2	19	38	26					
19*	41616	26 Oct 1972	7245.167	0.089720	65.7336	172.088	252.93	91.87	5068.760	0.2817	0.00121	0.00039	-	0.52	77	7.5	6595.13
			1	10	8	1	1	1	1	5	10	4					
20	41631	10 Nov 1972	7237.228	0.088756	65.7274	132.032	245.36	230.04	5077.104	0.2093	-			0.39	35	5.0	6594.88
			1	6	8	1	1	1	1	3							
21*	41644	23 Nov 1972	7231.415	0.088070	65.7305	97.215	238.72	29.79	5083.228	0.2838	0.00295	-		0.56	67	7.5	6594.54
			1	2	2	<1	1	1	1	2	11						
22	41660	9 Dec 1972	7222.561	0.087033	65.7366	54.227	230.58	77.81	5092.581	0.2740	-			0.48	45	7.1	6593.96
			<1	12	12	1	1	1	<1	2							
23	41679	28 Dec 1972	7211.535	0.085637	65.7405	2.969	220.81	110.28	5104.267	0.2293	-0.00075	-		0.64	68	6.9	6593.96
			1	19	16	2	1	1	1	3	13						
24*	41686	4 Jan 1973	7208.839	0.085279	65.7350	344.020	217.24	210.79	5107.130	0.1849	0.00794	-0.00049	-	0.54	90	5.3	6594.08
			1	15	3	1	1	1	1	11	26	16					
25*	41699	17 Jan 1973	7203.370	0.084581	65.7398	308.787	210.54	40.98	5112.950	0.1980	-0.00292	-		0.46	79	5.7	6594.10
			1	11	3	1	<1	<1	1	2	15						

Table 2 (continued)

	MJD	Date	a	e	i	Ω	ω	M_0	M_1	M_2	M_3	M_4	M_5	ε	N	D	a(1 − e)
26*	41712	30 Jan 1973	7197.766	0.083964	65.7372	273.468	203.81	306.61	5118.923	0.2429	-0.00333	-		0.54	69	5.6	6593.41
			1	18	7	1	1	1	1	4	23						
27	41739	26 Feb 1973	7181.911	0.081949	65.7294	199.766	189.78	124.26	5135.886	0.3962	-0.00120	0.00028	-	0.62	76	7.7	6593.36
			2	21	12	1	1	1	2	6	29	7					
28*	41749	8 Mar 1973	7174.605	0.080994	65.7353	172.330	184.62	42.50	5143.735	0.3841	-0.00502	-		0.42	81	5.4	6593.51
			<1	8	4	1	<1	<1	<1	2	8						
29	41760	19 Mar 1973	7166.919	0.080019	65.7353	142.040	178.84	149.64	5152.013	0.3901	0.01490	-0.00017	-0.00055	0.95	66	7.1	6593.43
			3	15	19	1	1	1	3	12	81	13	6				
30*	41769	28 Mar 1973	7160.820	0.079180	65.7292	117.181	174.14	109.08	5158.598	0.3092	-0.00228	-		0.72	91	4.0	6593.83
			<1	15	2	<1	<1	<1	<1	1	23						
31*	41772	31 Mar 1973	7159.221	0.079052	65.7277	108.880	172.55	107.55	5160.325	0.2766	-			0.53	53	3.1	6593.27
			2	20	9	2	1	1	2	11							
32	41779	7 Apr 1973	7154.727	0.078570	65.7261	89.483	168.88	247.61	5165.190	0.3211	-0.00070	-0.00063	-	0.53	89	5.9	6592.58
			1	18	10	2	1	1	1	10	23	14					
33*	41797	25 Apr 1973	7144.453	0.077165	65.7296	39.441	159.33	83.96	5176.338	0.2782	0.00933	-		0.58	42	4.8	6593.15
			2	18	10	1	1	1	2	6	44						
34	41806	4 May 1973	7139.215	0.076454	65.7239	14.341	154.54	256.40	5182.036	0.2811	0.00391	0.00386	-0.00137	0.79	45	5.3	6593.39
			4	25	18	2	1	1	4	24	200	43	24				
35	41826	24 May 1973	7128.206	0.075102	65.7251	318.348	143.90	336.75	5194.048	0.3107	-0.00917	0.00030	0.00021	0.81	49	7.7	6592.86
			2	13	11	1	1	1	2	9	65	7	4				
36*	41850	17 Jun 1973	7115.575	0.073476	65.7266	250.798	131.03	242.84	5207.887	0.2601	-			0.72	56	5.3	6592.75
			1	16	9	2	1	1	1	3							
37*	41859	26 Jun 1973	7111.572	0.072965	65.7255	225.368	126.24	334.10	5212.285	0.2280	-0.01194	-0.00054	0.00044	0.74	52	7.7	6592.68
			2	15	10	2	1	1	2	5	40	4	2				
38*	41889	26 Jul 1973	7102.681	0.071750	65.7253	140.361	110.07	259.93	5222.078	0.1704	0.00913	0.00134	-	0.72	55	6.2	6593.06
			1	2	9	2	2	1	1	10	12	12					
39	41917	23 Aug 1973	7093.597	0.070602	65.7212	60.701	94.86	103.42	5232.113	0.2054	0.01728	0.00092	-0.00084	0.76	60	5.6	6592.77
			3	11	17	2	1	1	3	12	151	21	17				
40*	41936	11 Sep 1973	7085.756	0.069660	65.7261	6.434	84.53	237.66	5240.802	0.2197	-0.00333	-0.00125	-	0.71	35	5.6	6592.16
			2	13	11	2	2	2	2	12	30	17					
41	41955	30 Sep 1973	7080.770	0.068793	65.7223	312.001	74.14	161.39	5248.564	0.2159	0.00003	0.00109	-	0.59	54	5.6	6591.80
			1	5	11	1	1	1	1	8	25	15					
42	41964	9 Oct 1973	7074.956	0.068265	65.7191	286.144	69.21	258.24	5252.809	0.2008	0.00132	0.00060	-	0.70	53	5.9	6591.98
			1	13	15	2	2	2	1	12	23	14					
43	41974	19 Oct 1973	7071.225	0.067798	65.7211	257.360	63.78	246.73	5256.968	0.2354	-0.00040	0.00055	-	0.84	69	5.5	6591.81
			1	13	16	2	2	2	2	13	31	19					
44	42001	15 Nov 1973	7058.489	0.066226	65.7215	179.355	48.99	182.34	5271.206	0.2326	-0.00329	-0.00187	0.00068	0.80	87	5.4	6591.03
			1	8	8	1	1	1	1	12	90	24	13				
45	42018	2 Dec 1973	7050.835	0.065291	65.7190	130.001	39.59	224.43	5279.793	0.2254	-0.00520	0.00044	0.00035	0.73	48	5.8	6590.48
			2	11	13	1	1	1	3	13	94	16	9				
46	42043	27 Dec 1973	7040.453	0.064012	65.7172	57.114	25.80	238.19	5291.478	0.2505	0.00345	0.00049	-	0.91	63	6.1	6589.78
			2	12	16	2	1	1	2	15	31	18					
47	42065	18 Jan 1974	7028.889	0.062494	65.7146	352.628	13.69	145.93	5304.544	0.3787	0.00117	-0.00040	-	0.85	58	6.0	6589.63
			2	23	18	1	2	1	2	15	29	17					
48*	42086	8 Feb 1974	7016.036	0.060898	65.7148	290.715	1.99	100.21	5319.130	0.3241	-0.00261	-	-	0.92	68	5.3	6588.77
			1	23	7	1	1	1	1	3	24						
49	42095	17 Feb 1974	7010.655	0.060343	65.7110	264.058	356.92	119.88	5325.256	0.3174	-0.00095	-	-	0.82	98	7.2	6587.61
			1	10	16	1	1	1	1	2	8						
50	42111	5 Mar 1974	7001.028	0.059078	65.7061	216.502	348.01	90.52	5336.245	0.3403	0.00176	0.00044	-	0.66	72	7.3	6587.42
			1	20	13	1	1	1	1	10	10	7					

Table 2 (continued)

	MJD	Date	a	e	i	Ω	ω	M_0	M_1	M_2	M_3	M_4	M_5	ε	N	D	a(1 - e)
51	42126	20 Mar 1974	6991.123	0.057812	65.7104	171.708	339.60	299.38	5347.593	0.3449	0.01520	0.00354	-0.00029	0.83	76	7.3	6586.95
			3	24	16	2	1	2	3	11	86	9	5				
52	42141	4 Apr 1974	6980.508	0.056477	65.7076	126.696	331.07	326.52	5359.797	0.4404	0.00702	-0.00133	-	0.53	50	5.6	6586.27
			1	14	12	1	1	1	1	15	28	19					
53	42146	9 Apr 1974	6976.805	0.055978	65.6995	111.635	328.25	136.37	5364.066	0.4192	0.00300	0.00199	-	0.76	68	3.9	6586.26
			2	29	14	2	2	2	2	26	68	67					
54	42156	19 Apr 1974	6969.039	0.055010	65.7010	81.434	322.51	181.24	5373.037	0.5275	0.00427	-0.00308	-	0.55	81	5.9	6585.67
			1	10	10	1	1	1	1	10	24	12					
55*	42164	27 Apr 1974	6962.938	0.054206	65.7046	57.193	317.93	355.70	5380.101	0.3923	0.00628	-0.00340	-0.00154	0.46	94	4.2	6585.50
			2	12	5	1	1	1	2	17	173	53	36				
56	42172	5 May 1974	6957.488	0.053598	65.7066	32.883	313.32	221.01	5386.426	0.4450	-0.00260	-0.00123	0.00011	0.64	80	7.6	6584.58
			2	16	13	1	2	2	2	7	51	5	3				
57	42191	24 May 1974	6946.439	0.052120	65.7003	334.911	302.41	96.75	5399.284	0.2556	0.00693	-0.00091	-0.00056	0.38	69	5.9	6584.39
			1	9	8	1	1	1	2	7	66	9	6				
58	42212	14 Jun 1974	6936.988	0.050902	65.7027	270.534	290.31	193.72	5410.325	0.2742	-0.00380	0.00121	-0.00017	0.45	68	7.2	6583.88
			1	8	11	1	2	2	1	8	46	8	3				
59*	42219	21 Jun 1974	6933.951	0.050514	65.7026	249.010	286.24	278.81	5413.880	0.2412	-0.00324	-0.00096	-	0.41	74	5.8	6583.69
			1	6	4	1	1	1	<1	4	10	7					
60	42230	2 Jul 1974	6929.254	0.049887	65.6986	215.123	279.85	100.37	5419.387	0.2473	-0.00233	0.00087	0.00019	0.42	72	7.9	6583.57
			1	7	9	1	1	1	1	7	36	5	2				
61	42246*	18 Jul 1974	6921.579	0.048938	65.6994	165.679	270.62	127.26	5428.406	0.2159	-0.00534	0.00005	0.00011	0.60	100	7.6	6582.85
			2	9	8	1	2	2	2	7	45	6	3				
62	42253*	25 Jul 1974	6918.709	0.048559	65.7015	143.995	266.51	336.64	5431.784	0.2984	-0.02584	-0.00094	0.00147	0.54	71	5.3	6582.74
			2	10	7	1	2	2	3	13	141	29	18				
63	42260	1 Aug 1974	6915.862	0.048205	65.7007	122.281	262.48	211.17	5435.139	0.2123	0.00197	0.00149	-	0.51	90	5.9	6582.48
			1	9	10	1	2	2	1	10	16	10					
64	42268	9 Aug 1974	6912.330	0.047758	65.6991	97.427	257.80	149.02	5439.307	0.2613	0.00119	-0.00078	-	0.57	84	6.8	6582.21
			1	10	12	1	2	2	1	9	14	8					
65	42291	1 Sep 1974	6900.678	0.046222	65.6971	25.716	244.50	120.10	5453.091	0.3615	0.00627	0.00016	-0.00019	0.30	58	7.6	6581.71
			1	7	8	1	1	1	1	5	27	4	2				
66	42307	17 Sep 1974	6889.308	0.044810	65.7039	335.558	235.09	350.06	5466.600	0.5569	-0.01235	-0.00092	0.00062	0.92	62	7.7	6580.60
			3	23	19	2	3	4	4	15	89	10	5				
67	42319	29 Sep 1974	6879.090	0.043597	65.7000	297.741	228.10	143.89	5478.787	0.4759	0.00091	0.00133	-	0.64	80	7.8	6579.18
			1	14	13	2	2	2	1	7	14	6					
68	42329	9 Oct 1974	6870.166	0.042337	65.6962	266.068	222.29	263.28	5489.467	0.6731	0.03047	-0.00252	-0.00127	0.58	77	6.6	6579.30
			2	17	9	1	2	2	3	11	85	11	6				
69	42344	24 Oct 1974	6852.653	0.040101	65.6968	218.251	213.39	331.39	5510.530	0.5587	0.01959	0.00105	-0.00071	0.55	59	7.6	6577.85
			2	17	14	2	2	2	3	9	57	6	3				
70	42362	11 Nov 1974	6832.209	0.037369	65.6917	160.364	203.00	8.78	5535.287	0.8884	0.00419	-		0.88	62	7.4	6576.90
			2	17	24	2	3	3	2	3	22						
71	42377	26 Nov 1974	6812.269	0.034751	65.6846	111.610	193.77	63.62	5559.612	0.8531	0.00095	-0.00075	0.00008	0.65	87	7.8	6575.54
			1	17	9	1	2	2	2	7	37	4	2				
72	42390	9 Dec 1974	6794.376	0.032383	65.6868	68.966	185.84	122.96	5581.593	0.8182	0.01348	-0.00044	-0.00044	0.64	73	7.6	6574.35
			2	12	10	1	2	2	2	8	53	5	3				
73	42398	17 Dec 1974	6783.746	0.030927	65.6860	42.538	180.77	188.82	5594.721	0.8522	0.02166	0.00152	-0.00034	0.71	77	7.6	6573.95
			2	16	11	1	2	2	2	9	48	6	3				
74	42413	1 Jan 1975	6762.753	0.028166	65.6774	352.557	171.39	76.27	5620.798	0.7019	-0.00369	-0.00010	-	0.75	58	7.8	6572.27
			1	26	16	1	3	3	1	13	12	8					
75	42424	12 Jan 1975	6749.215	0.026282	65.6821	315.608	164.32	76.82	5637.722	0.7013	-0.00165	0.00509	0.00101	0.62	61	7.0	6571.83
			2	22	16	2	3	3	2	16	105	12	8				

Table 2 (concluded)

	MJD	Date	a	e	i	Ω	ω	M_0	M_1	M_2	M_3	M_4	M_5	ε	N	D	a(1 − e)
76	42438	26 Jan 1975	6731.372	0.023941	65.6737	268.165	155.24	327.55	5660.158	0.7093	−0.00185	0.00312	0.00021	0.50	63	7.0	6570.22
			2	17	12	2	3	3	2	7	63	7	4				
77	42448	5 Feb 1975	6718.089	0.022146	65.6664	234.053	148.53	129.40	5676.956	0.9131	0.00111	0.00121	-	0.83	83	7.5	6569.31
			1	9	7	1	2	2	1	9	12	7					
78	42457	14 Feb 1975	6703.003	0.020218	65.6642	203.099	142.43	184.07	5696.137	1.1440	−0.01118	0.00020	0.00026	0.62	64	7.2	6567.48
			1	14	12	1	5	5	2	10	57	10	4				
79	42468	25 Feb 1975	6684.753	0.017818	65.6683	164.939	134.65	332.70	5719.484	1.0889	−0.00727	−0.00310	0.00020	0.51	63	7.1	6565.64
			2	18	14	2	5	4	2	10	59	8	4				
80	42478	7 Mar 1975	6667.741	0.015782	65.6710	129.942	126.95	33.31	5741.392	1.3256	−0.03073	−0.00987	0.00196	0.74	53	5.6	6562.51
			2	12	17	2	9	8	2	12	114	17	13				
81	42484	13 Mar 1975	6653.966	0.014201	65.6572	108.775	122.37	330.37	5759.234	1.6950	−0.02065	0.00577	-	0.74	54	5.8	6559.47
			2	16	21	2	6	6	2	16	38	22					
82	42490	19 Mar 1975	6637.953	0.012374	65.6612	87.431	117.75	28.11	5780.091	1.8347	0.03097	0.00126	−0.00134	0.54	37	5.7	6555.81
			3	18	19	2	12	12	4	17	142	20	13				
83	42496	25 Mar 1975	6619.997	0.010263	65.6585	65.896	112.65	218.07	5803.630	2.3484	0.03972	−0.00125	0.00218	0.86	30	5.9	6552.06
			7	20	15	1	13	12	9	42	325	40	27				
84	42501	30 Mar 1975	6596.460	0.008059	65.6467	47.769	108.59	146.56	5834.727	3.8942	0.05641	0.05033	-	0.81	16	2.9	6543.30
			6	24	30	3	31	31	8	84	1013	562					
85	42505	3 Apr 1975	6563.488	0.005051	65.6493	33.056	104.89	163.02	5878.759	8.5625	1.14266	0.30084	0.05230	0.71	39	2.5	6530.34
			10	22	18	3	25	25	13	270	1917	3118	1488				

* Orbits using Hewitt camera observations

Key:

MJD = modified Julian day

a = semi major axis (km)

e = eccentricity

i = inclination (deg)

Ω = right ascension of ascending node (deg)

ω = argument of perigee (deg)

M_0 = mean anomaly at epoch (deg)

M_1 = mean motion n (deg/day)

M_2, M_3, M_4, M_5 = later coefficients in the polynomial for M

ε = measure of fit

N = number of observations used

D = time covered by the observations (days)

Table 4

THE 15 DAILY SETS OF ORBITAL PARAMETERS BEFORE DECAY, WITH STANDARD DEVIATIONS

	MJD	Date	a	e	i	Ω	ω	M_0	M_1	M_2	M_3	M_4	ε	N	D	a(1 − e)
A	42492	21 Mar 1975	6632.096	0.011667	65.6593	80.283	116.02	76.23	5787.752	1.997			0.83	86	1.44	6554.72
			2	7	7	1	7	7	3	7						
B	42493	22 Mar 1975	6629.271	0.011345	65.6586	76.697	115.26	106.00	5791.453	1.772			0.91	100	0.94	6554.06
			2	10	9	1	6	5	3	9						
C	42494	23 Mar 1975	6626.661	0.011060	65.6567	73.106	114.47	139.32	5794.875	1.878	0.41		0.91	100	0.93	6553.37
			5	10	8	1	7	7	6	10	4					
D	42495	24 Mar 1975	6623.514	0.010745	65.6560	69.508	113.65	176.42	5799.007	1.970			0.73	46	0.80	6552.34
			4	13	13	2	9	9	5	14						
E	42496	25 Mar 1975	6619.992	0.010386	65.6562	65.909	112.66	217.94	5803.636	2.706			0.49	78	0.80	6551.24
			2	6	10	1	4	4	3	14						
F	42497	26 Mar 1975	6616.291	0.009949	65.6559	62.300	112.31	263.78	5808.507	2.413			0.94	79	0.80	6550.47
			3	11	15	1	10	10	4	14						
G	42498	27 Mar 1975	6612.384	0.009636	65.6550	58.679	111.14	315.27	5813.658	2.794			0.93	79	0.93	6548.67
			3	12	14	2	12	11	4	14						
H	42499	28 Mar 1975	6607.772	0.009124	65.6559	55.054	110.45	11.82	5819.747	3.516			1.04	94	0.99	6547.48
			2	11	9	2	13	13	3	11						
I	42500	29 Mar 1975	6602.256	0.008580	65.6558	51.424	109.60	75.35	5827.044	3.758			0.84	100	0.86	6545.61
			2	8	8	1	8	8	3	11						
J	42501	30 Mar 1975	6596.466	0.008049	65.6563	47.773	109.26	145.87	5834.719	3.936			0.96	96	0.93	6543.37
			2	11	11	1	8	8	3	11						
K	42502	31 Mar 1975	6590.346	0.007515	65.6563	44.118	107.91	225.29	5842.850	4.364	0.44		0.75	77	0.92	6540.82
			7	13	8	1	11	11	9	11	5					
L	42503	1 Apr 1975	6583.083	0.006914	65.6532	40.450	107.00	313.05	5852.525	5.356			0.79	92	0.92	6537.57
			3	8	11	1	9	9	3	11						
M	42504	2 Apr 1975	6574.476	0.006177	65.6555	36.759	106.11	51.41	5864.025	6.194	0.63		0.82	51	0.80	6533.87
			5	13	14	2	13	13	7	47	10					
N	42505	3 Apr 1975	6563.409	0.005188	65.6542	33.060	106.10	161.83	5878.865	8.756			0.59	72	0.63	6529.36
			2	7	7	2	16	16	3	21						
O	42506	4 Apr 1975	6546.778	0.003945	65.6518	29.325	103.13	292.99	5901.288	14.992	3.77	3.97	0.93	88	0.88	6520.95
			5	8	8	2	22	22	7	77	5	38				

Key:
- MJD = modified Julian day
- a = semi major axis (km)
- e = eccentricity
- i = inclination (deg)
- Ω = right ascension of ascending node (deg)
- ω = argument of perigee (deg)
- M_0 = mean anomaly at epoch (deg)
- M_1 = mean motion n (deg/day)
- M_2, M_3, M_4 = later coefficients in the polynomial for M
- ε = measure of fit
- N = number of observations used
- D = time covered by the observations (days)

REFERENCES

No.	Author	Title, etc
1	L. Freedman	The Soviet Union and anti-space defence. *Survival*, XIX, No.1, 16-23 (1977)
2	G.E. Perry	Russian hunter-killer satellite experiments. *Royal Air Forces Quarterly*, Vol 17 (Winter 1977)
3	C.S. Sheldon II	*Soviet Space Program, 1971-75* Vol 1, pp 424-429. US Govt Printing Office, Washington (1976)
4	J.A. Pilkington D.G. King-Hele H. Hiller	Table of Earth satellites, Vol 2: 1969-1973. RAE Technical Report 74105 (1974)
5	R.H. Gooding R.J. Tayler	A PROP 3 users' manual. RAE Technical Report 68299 (1968)
6	R.H. Gooding	The evolution of the PROP 6 orbit determination program, and related topics. RAE Technical Report 74164 (1974)
7	D.M.C. Walker	Variations in air density from January 1972 to April 1975 at heights near 200 km. *Planet. Space Sci.*, 26, 291-309 (1978) RAE Technical Report 77078 (1977)
8	D.G. King-Hele G.E. Cook	Analysis of 27 satellite orbits to determine odd zonal harmonics in the geopotential. *Planet. Space Sci.*, 22, 645-672 (1974) RAE Technical Report 73153 (1973)
9	D.W. Scott	ORES: a computer program for the analysis of residuals from PROP. RAE Technical Report 69163 (1969)
10	W.M. Kaula	*Theory of satellite geodesy.* Blaisdell; Waltham, Mass. (1966)
11	R.H. Gooding	Studies of resonance in the orbits of Ariel satellites. RAE Technical Report (to be issued)

REFERENCES (continued)

No.	Author	Title, etc
12	R.R. Allan	Resonance effect on inclination for close satellites. RAE Technical Report 71245 (1971) (Also *Planet. Space Sci.*, 21, 205-225 (1973))
13	J. Klokočnik	Changes of the inclination of a close Earth satellite due to orbital resonances. *Bulletin of Astronomical Institutes of Czechoslovakia*, 27, 287-295 (1976)
14	D.G. King-Hele D.M.C. Walker R.H. Gooding	Evaluation of 14th-order harmonics in the geopotential. RAE Technical Report 78015 (1978)
15	R.H. Gooding	Lumped geopotential coefficients $\bar{C}_{15,15}$ and $\bar{S}_{15,15}$ obtained from resonant variation in the orbit of Ariel 3. RAE Technical Report 71068 (1971)
16	G.E. Cook	PROD, a computer program for predicting the development of drag-free satellite orbits. Part 1: theory. RAE Technical Report 71007 (1971) (*Celestial Mechanics*, 7, 301-314 (1973))
17	D.M.C. Walker	Analysis of the orbit of Ariel 1, 1962-15A, near 15th-order resonance. *Planet. Space Sci.*, 23, 565-574 (1975) RAE Technical Report 74107 (1974)
18	D.M.C. Walker	29th-order harmonics in the geopotential from the orbit of Ariel 1 at 29:2 resonance. *Planet. Space Sci.*, 25, 337-342 (1977) RAE Technical Report 76110 (1976)
19	D.G. King-Hele	Analysis of the orbit of Cosmos 387 (1970-111A) near 15th-order resonance. *Planet. Space Sci.*, 22, 509-524 (1974) RAE Technical Report 73132 (1973)
20	H. Hiller	The orbit of the satellite 1968-86A. RAE Technical Report 72147 (1972)

089

REFERENCES (continued)

No.	Author	Title, etc
21	D.G. King-Hele D.M.C. Walker R.H. Gooding	Geopotential harmonics of order 15 and odd degree from analysis of resonant orbits. *Planet. Space Sci.*, 23, 1239-1256 (1975) RAE Technical Report 75006 (1975)
22	D.G. King-Hele D.M.C. Walker R.H. Gooding	Geopotential harmonics of order 15 and even degree from changes in orbital eccentricity at resonance. *Planet. Space Sci.*, 23, 229-246 (1975) RAE Technical Report 74120 (1974)
23	D.G. King-Hele D.W. Scott	A revaluation of the rotational speed of the upper atmosphere. *Planet. Space Sci.*, 14. 1339-1365 (1966) RAE Technical Report 66189 (1966)
24	D.G. King-Hele	The effect of a meridional wind on a satellite orbit. *Proc. Roy. Soc. A*, 294, 261-272 (1966) RAE Technical Report 66010 (1966)
25	T.L. Felsentreger J.G. March R.W. Agreen	Analyses of the solid Earth and ocean tidal perturbations on the orbits of the Geos 1 and Geos 2 satellites. *Journ. Geophys. Res.*, 81, 2557-2563 (1976)
26	J.W. Slowey	Systematic winds at heights between 350 and 675 km from analysis of the orbits of four balloon satellites. *Planet. Space Sci.*, 23, 879-886 (1975)
27	P.W. Blum I. Harris	The global wind system in the thermosphere. *Space Research XIII*, pp 369-375, Akademie-Verlag, Berlin (1972)
28	B.K. Ching J.M. Straus	Ionospheric model effects on thermospheric calculations. *Journ. Atmos. Terr. Phys.*, 39, 1389-1394 (1977)
29	P.W. Blum I. Harris	Full non-linear treatment of the global thermospheric wind system - II. Results and comparison with observations. *Journ. Atmos. Terr. Phys.*, 37, 213-235 (1975)
30	R.M. Harper	Tidal winds in the 100- to 200-km region at Arecibo. *Journ. Geophys., Res.*, 82, 3243-3250 (1977)

089

REFERENCES (continued)

No.	Author	Title, etc
31	D.A. Antoniadis	Thermospheric winds and exospheric temperatures from incoherent scatter radar measurements in four seasons. *Journ. Atmos. Terr. Phys.*, 38, 187-195 (1976)
32	P. Amayenc	Tidal oscillations of the meridional neutral wind at midlatitudes. *Radio Science*, 9, 281-293 (1974)
33	D.G. King-Hele D.M.C. Walker	Upper-atmosphere zonal winds: variation with height and local time. *Planet. Space Sci.*, 25, 313-336 (1977) RAE Technical Report 76055 (1976)
34	D.M.C. Walker	Upper-atmosphere winds from the orbit of 1973-101A. *Journ. Brit. Interplan. Soc.*, 31, 197-199 (1978) RAE Technical Memorandum Space 254 (1977)
35	D.G. King-Hele D.W. Scott	The effect of atmospheric rotation on a satellite orbit, when scale height varies with height. *Planet. Space Sci.*, 17, 217-232 (1969) RAE Technical Report 68066 (1968)
36	G. Hernandez R.G. Roble	Direct measurements of nighttime thermospheric winds and temperatures 1. Seasonal variations during geomagnetic quiet periods. *Journ. Geophys. Res.*, 81, 2065-2074 (1976)
37	R.G. Roble J.E. Salah B.A. Emery	The seasonal variation of the diurnal thermospheric winds over Millstone Hill during solar cycle maximum. *Journ. Atmos. Terr. Phys.*, 39, 503-511 (1977)
38	D.M.C. Walker	Analysis of the orbit of 1970-65D, Cosmos 359 rocket. *Planet. Space Sci.*, 22, 391-402 (1974) RAE Technical Report 73110 (1973)
39	H. Hiller	Analysis of the orbit of 1970-97B (Cosmos 378 rocket). *Planet. Space Sci.*, 23, 1369-1376 (1975) RAE Technical Report 74161 (1974)

REFERENCES (concluded)

No.	Author	Title, etc
40	H. Hiller	Determination and geophysical interpretation of the orbit of China 2 rocket (1971-18B). RAE Technical Report 78107 (1978)
41	D.G. King-Hele D.M.C. Walker	Air density at heights near 150 km in 1970, from the orbit of Cosmos 316 (1969-108A). *Planet. Space Sci.*, 19, 1637-1651 (1971). RAE Technical Report 71129 (1971)
42	D.G. King-Hele G.E. Cook D.M.C. Walker	The contraction of satellite orbits under the influence of air drag. Part II: With oblate atmosphere. RAE Technical Note GW 565 (1960) (*Proc. Roy. Soc. A*, 264, 88-121 (1961))
43	D.G. King-Hele G.E. Cook	The contraction of satellite orbits under the influence of air drag. Part IV: With scale height dependent on altitude. RAE Technical Note Space 18 (1962) (*Proc. Roy. Soc. A*, 275, 357-390 (1963))
44	-	*CIRA 1972* (COSPAR International Reference Atmosphere 1972). Akademie-Verlag, Berlin (1972)

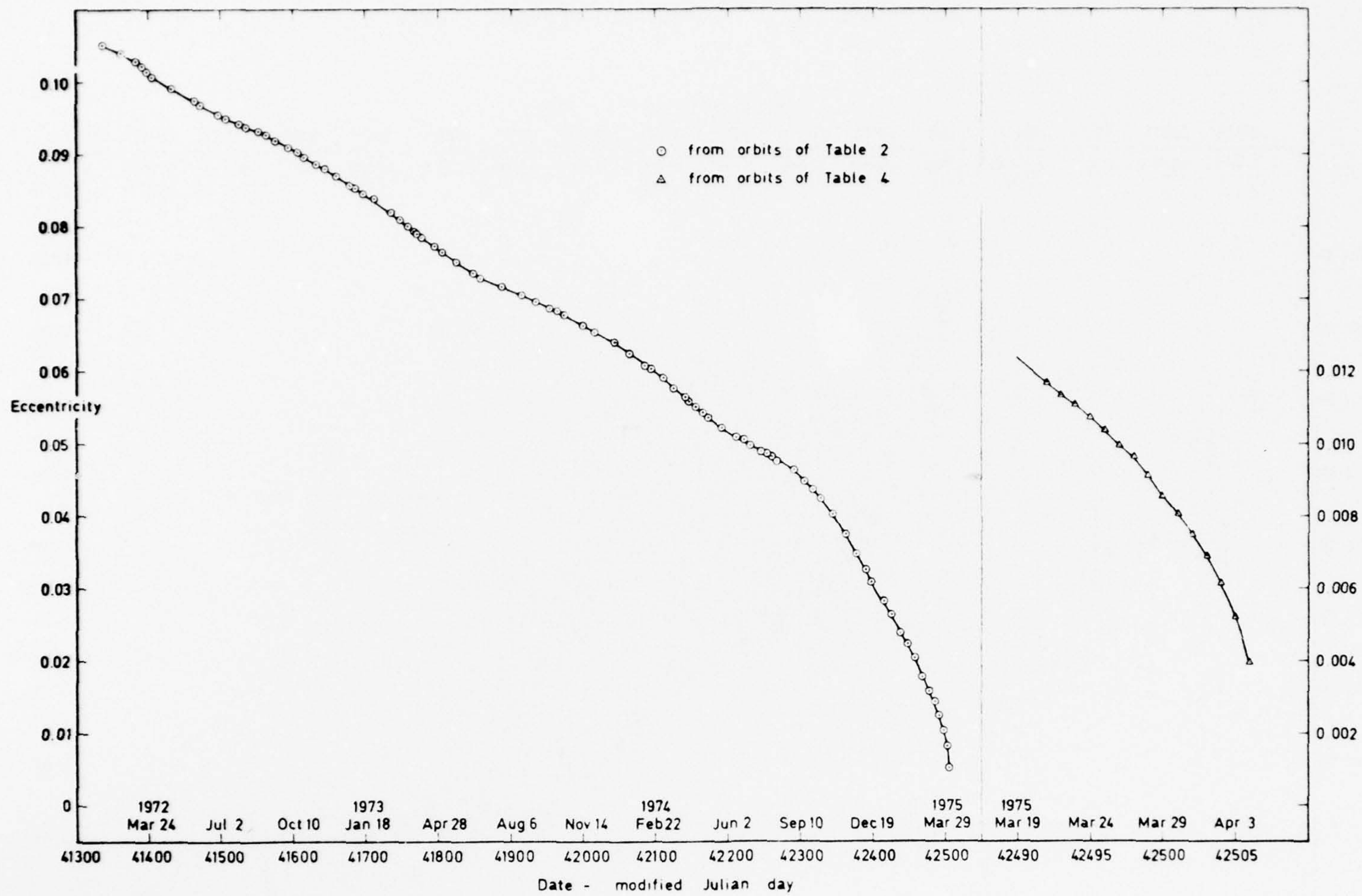

Fig 1 Variation of eccentricity, e, for Cosmos 462

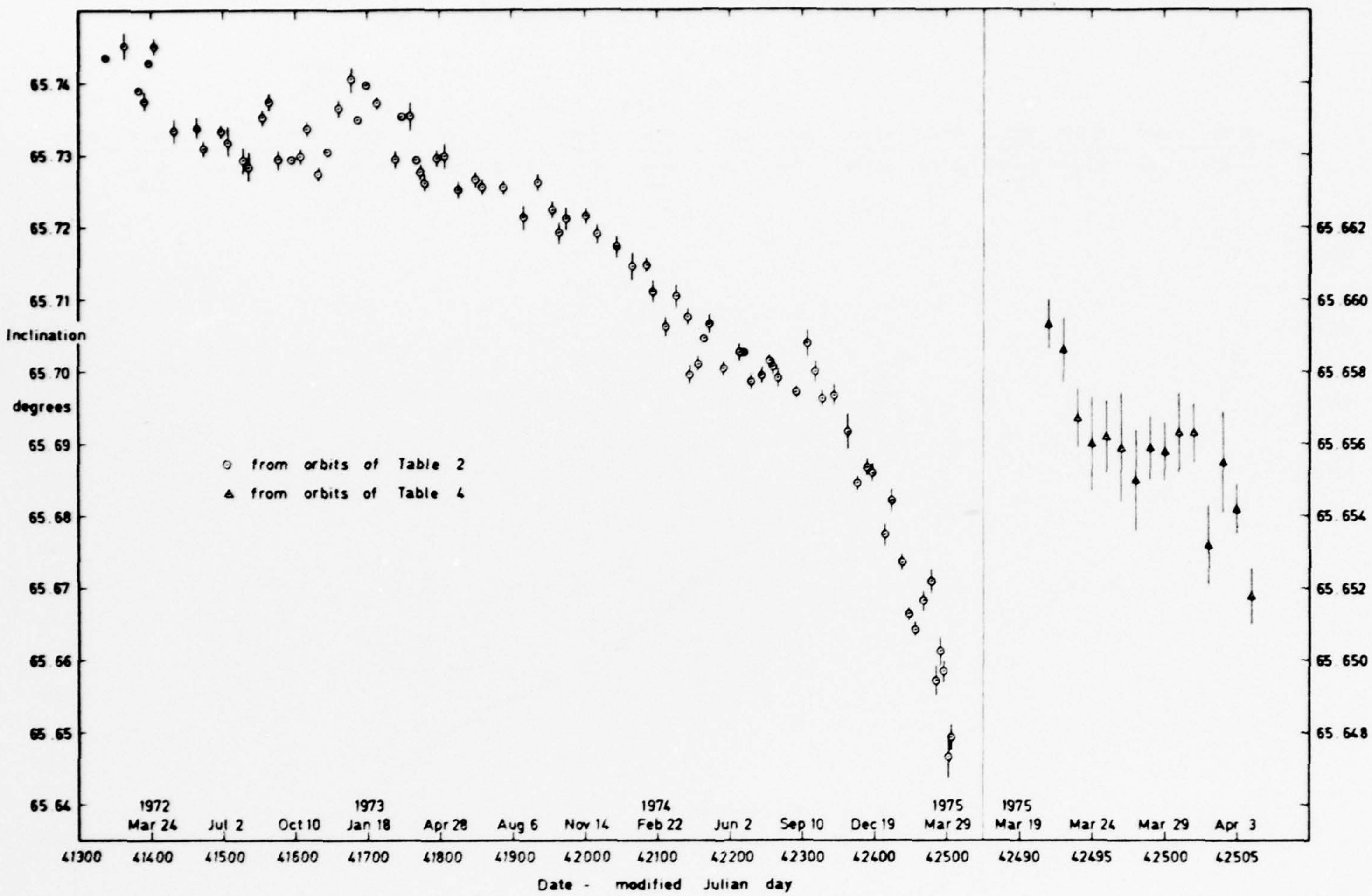

Fig 2 Variation of inclination, i, for Cosmos 462

TR 78089

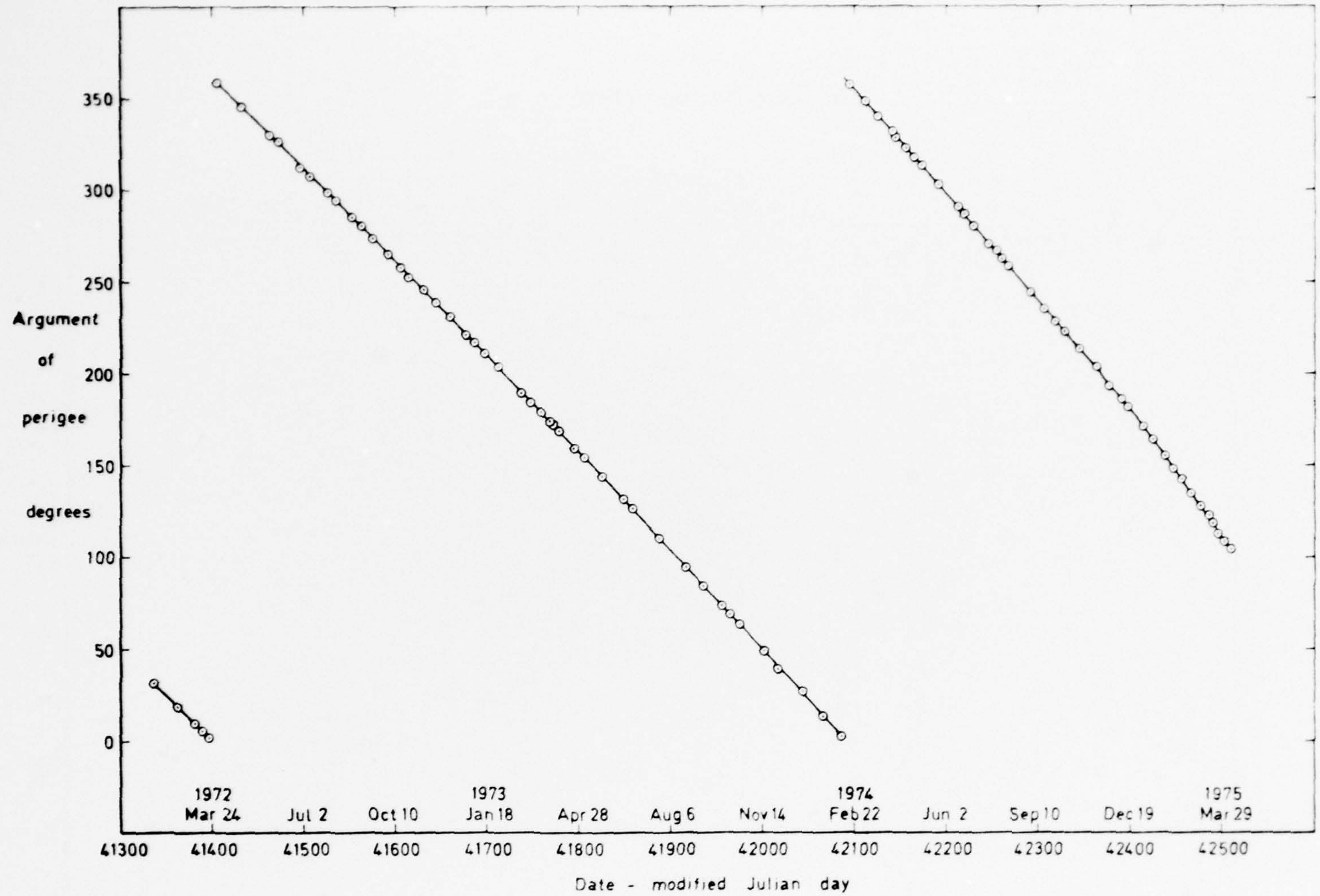

Fig 3 Variation of argument of perigee, ω, for Cosmos 462

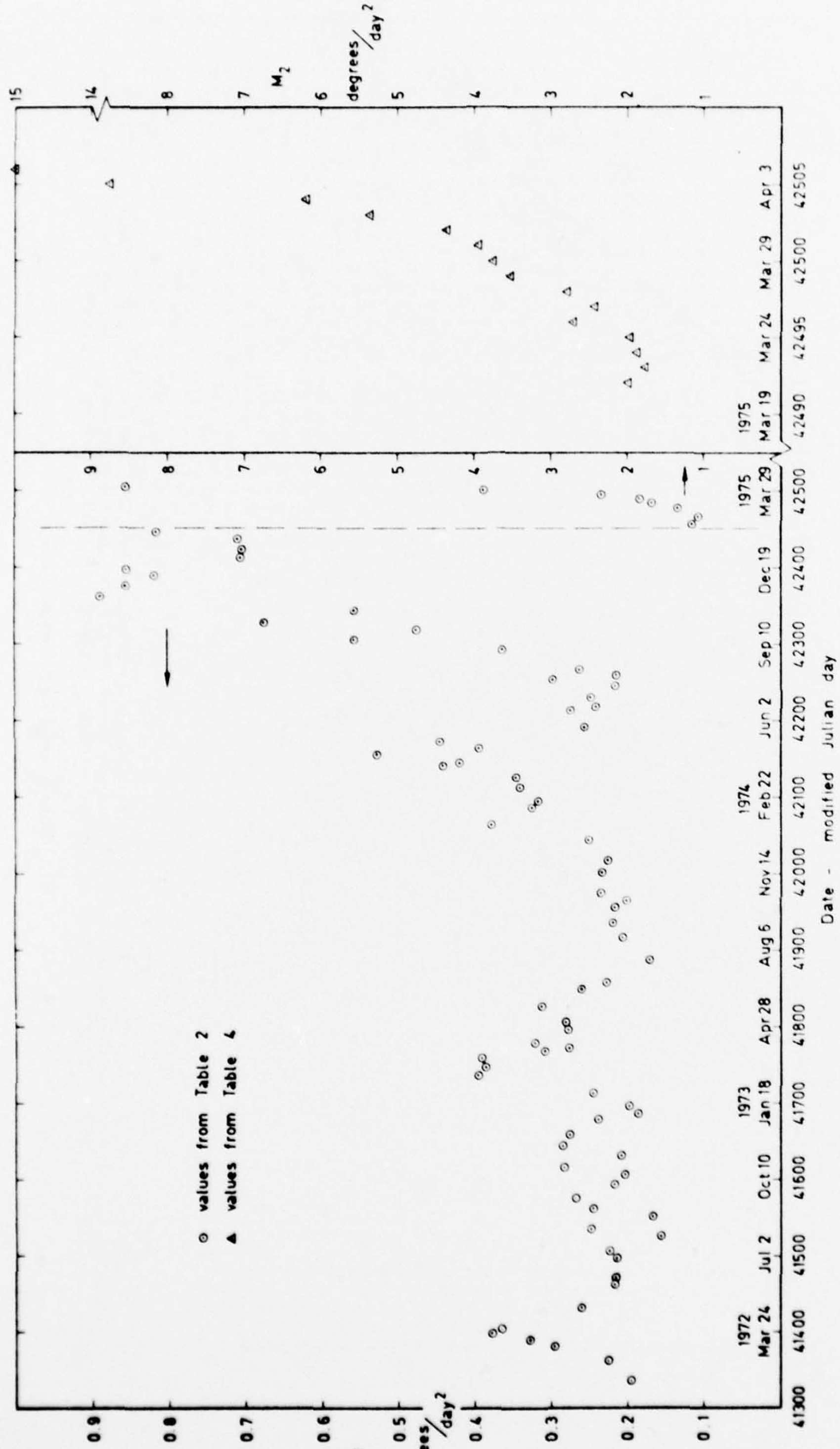

Fig 4 Values of M_2 for Cosmos 462

TR 78089

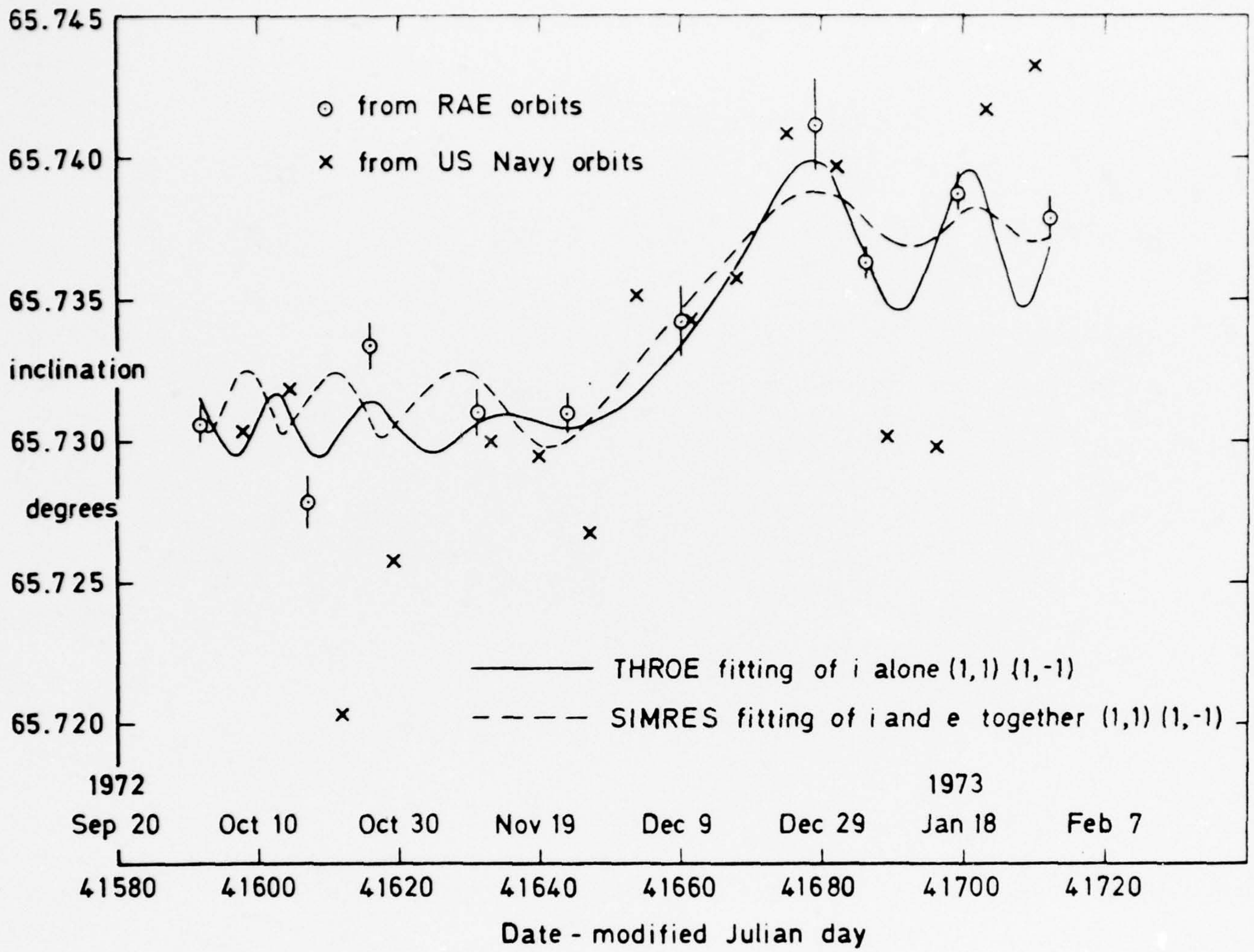

Fig 5 Variation of inclination at 14th-order resonance

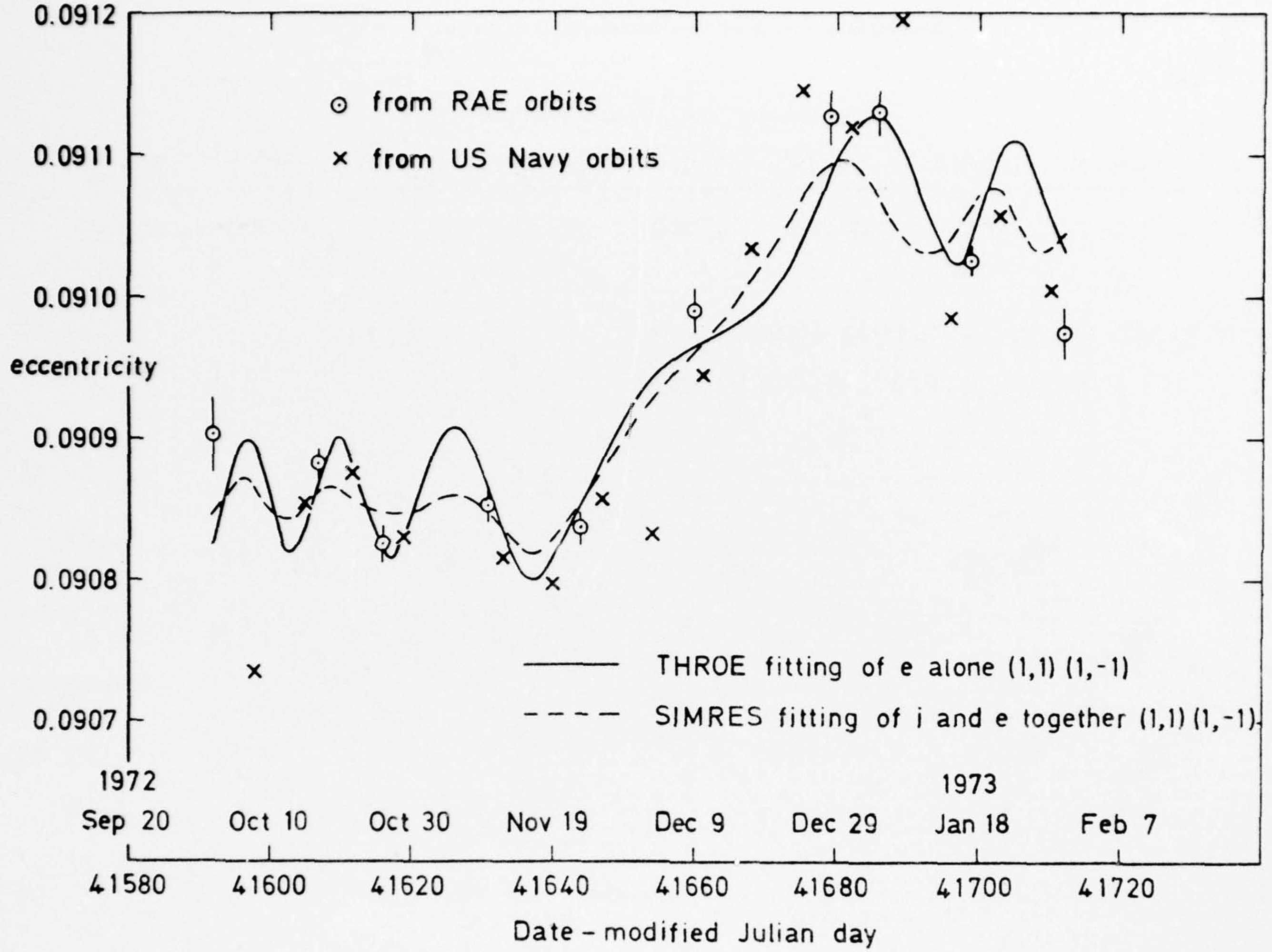

Fig 6 Variation of eccentricity at 14th-order resonance

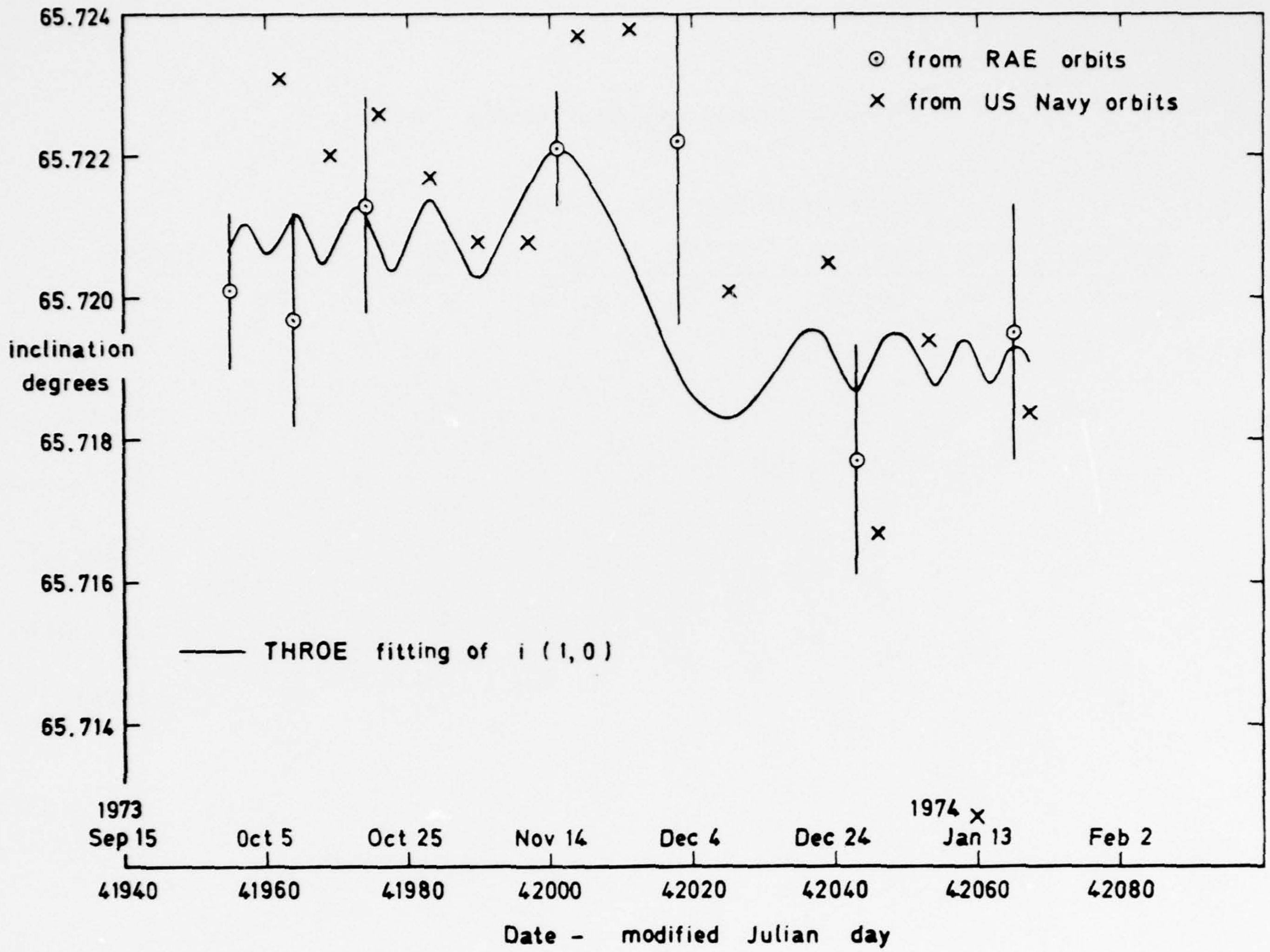

Fig 7 Variation of inclination at 29:2 resonance

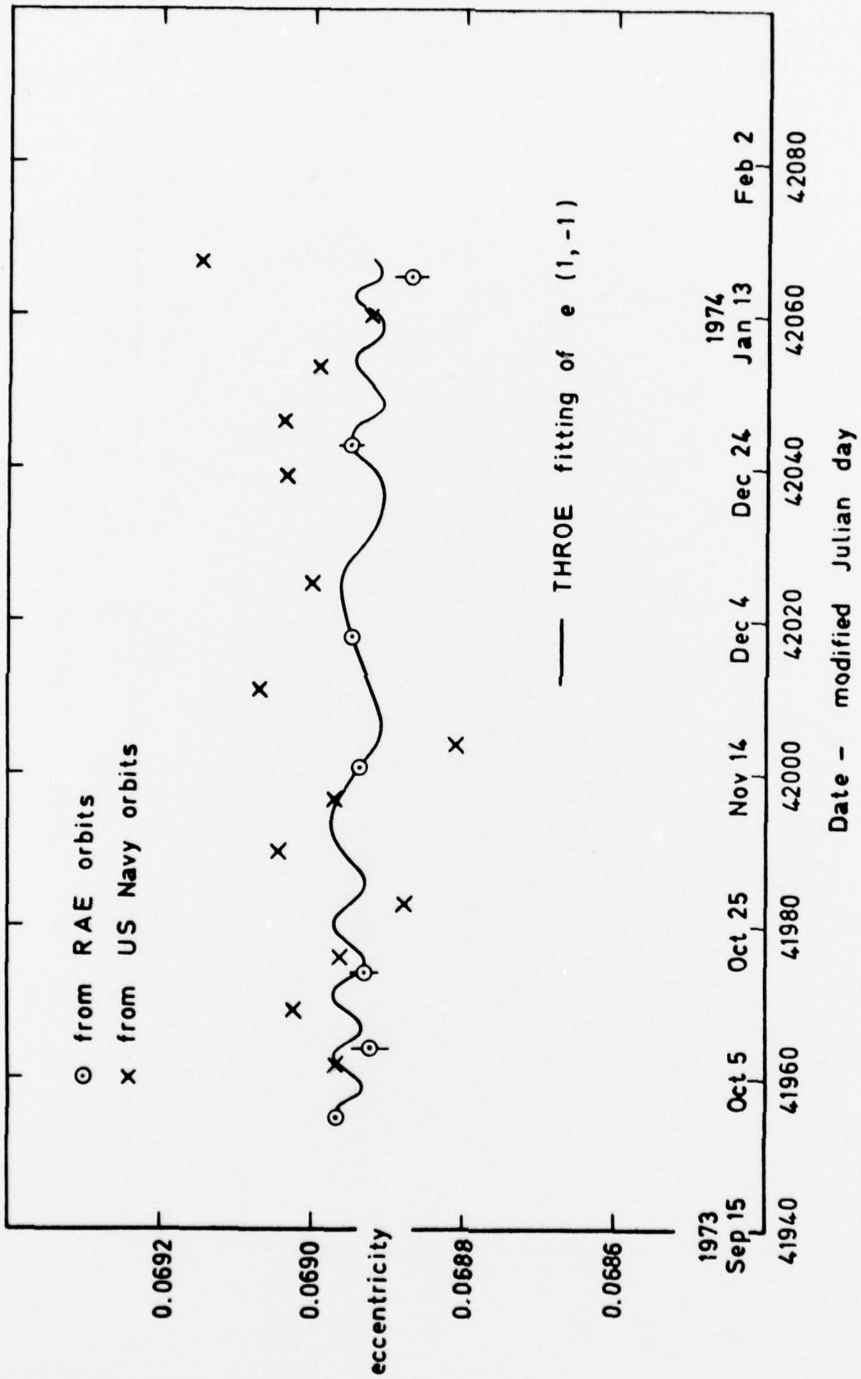

Fig 8 Variation of eccentricity at 29:2 resonance

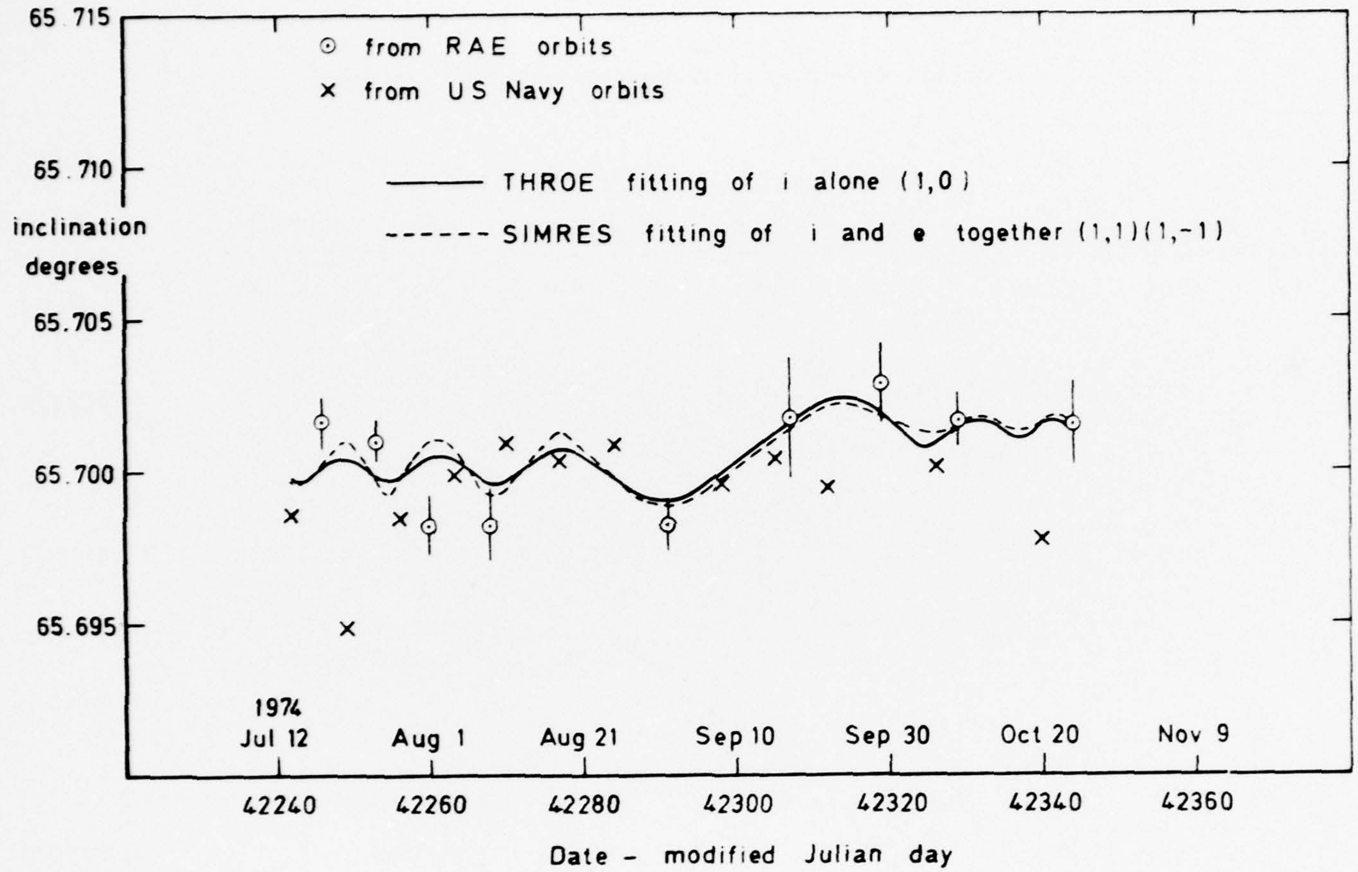

Fig 9 Variation of inclination at 15th-order resonance

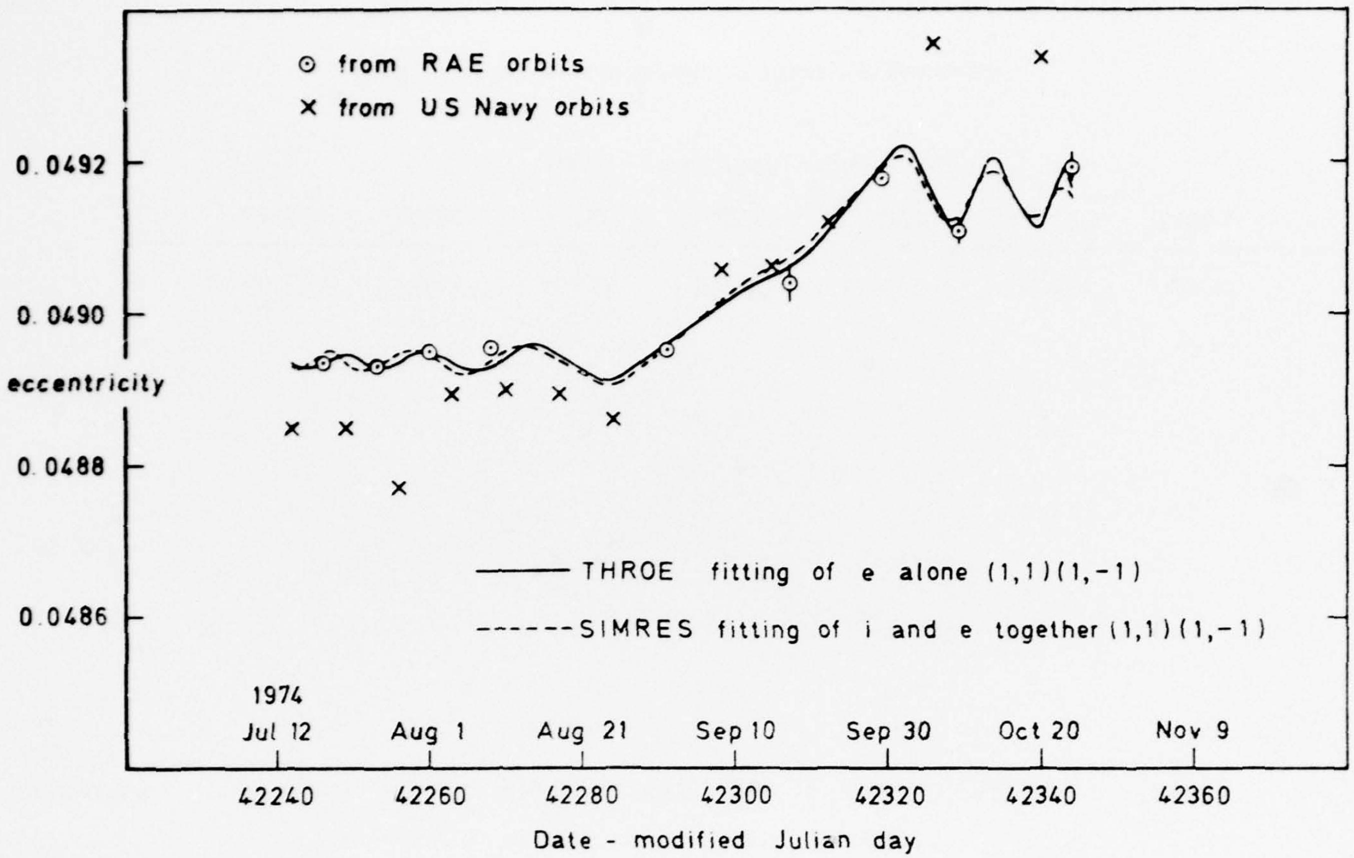

Fig 10 Variation of eccentricity at 15th-order resonance

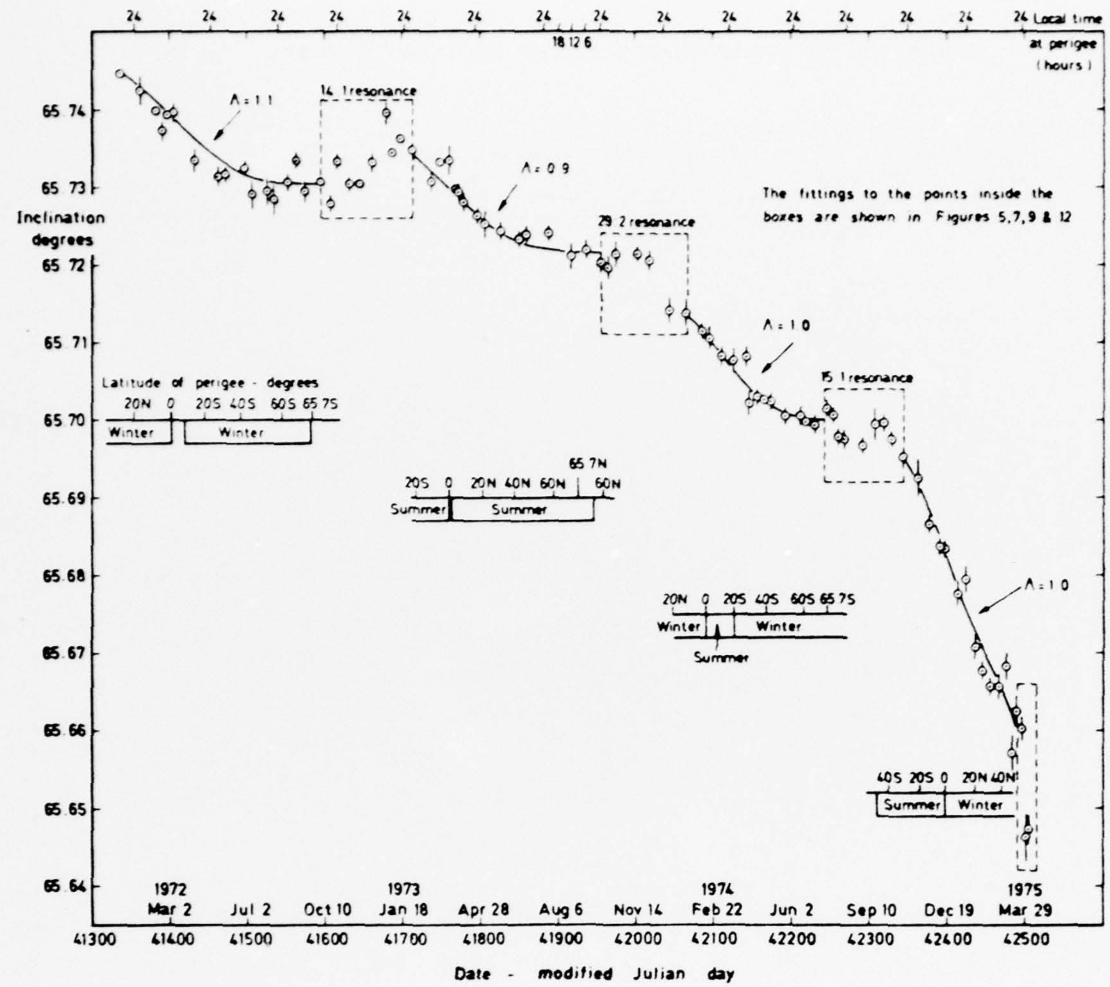

Fig 11 Values of inclination cleared of perturbations

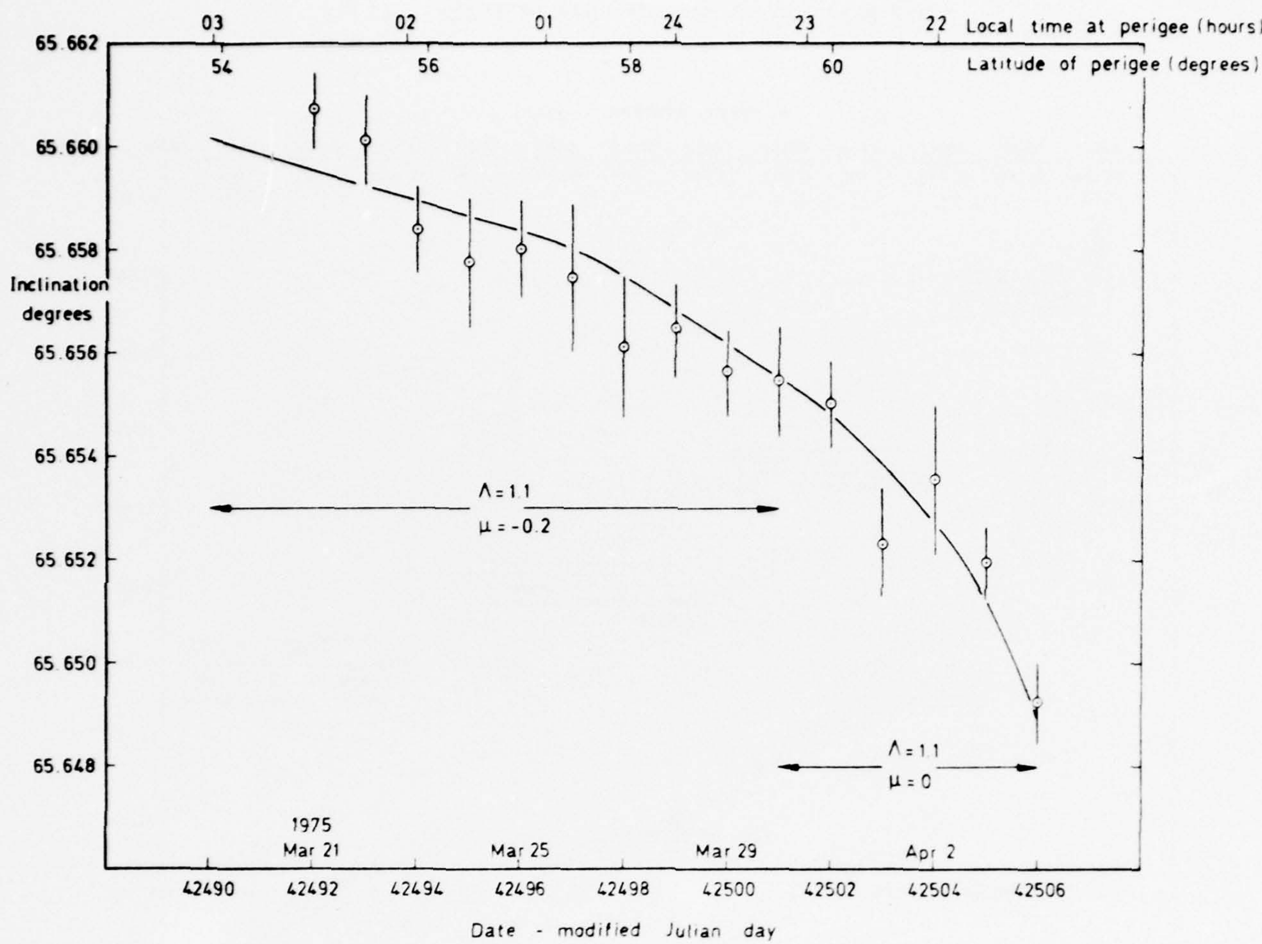

Fig 12 Values of inclination, cleared of perturbations, for last 15 days

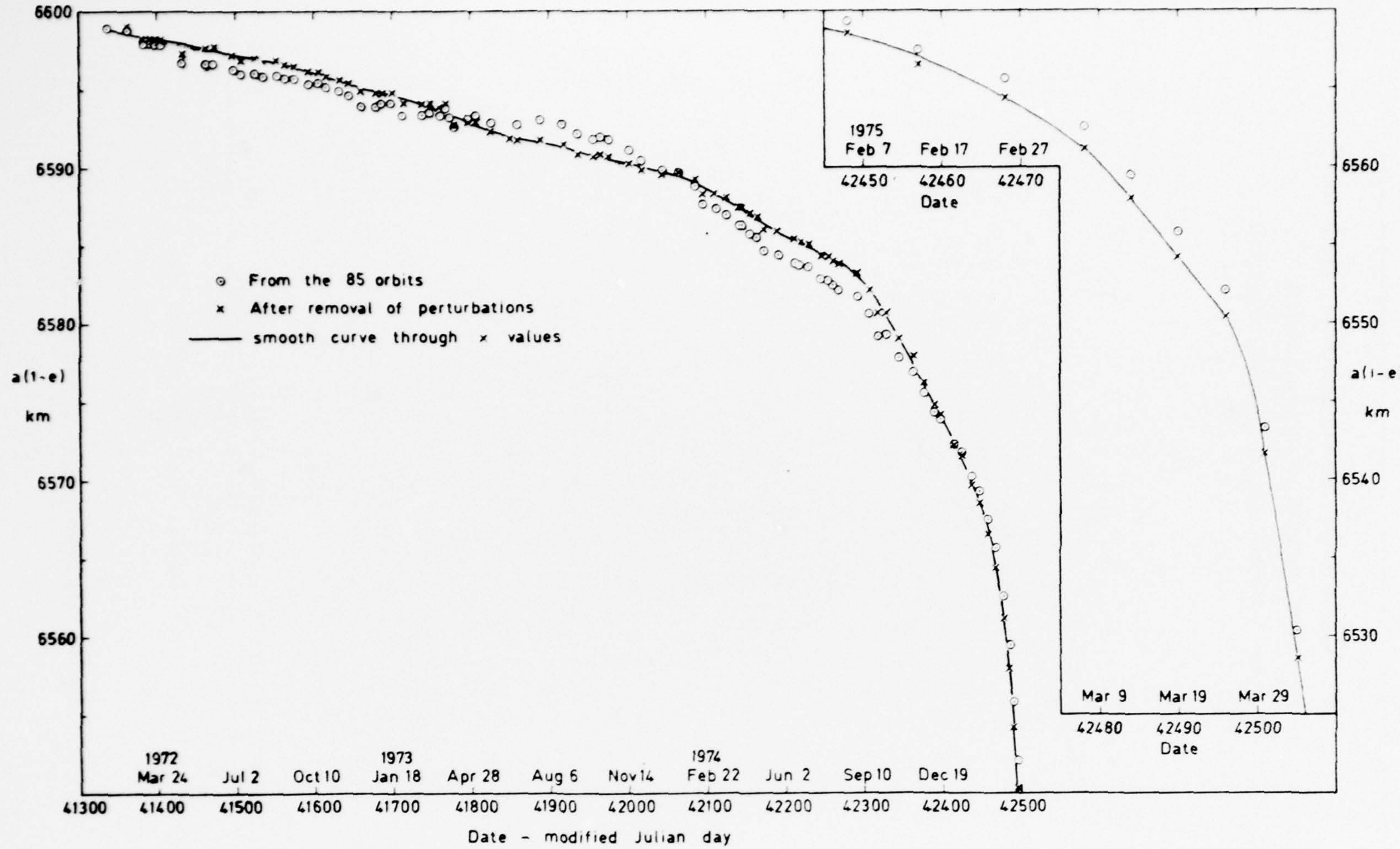

Fig 13 Values of a(1 – e) for Cosmos 462

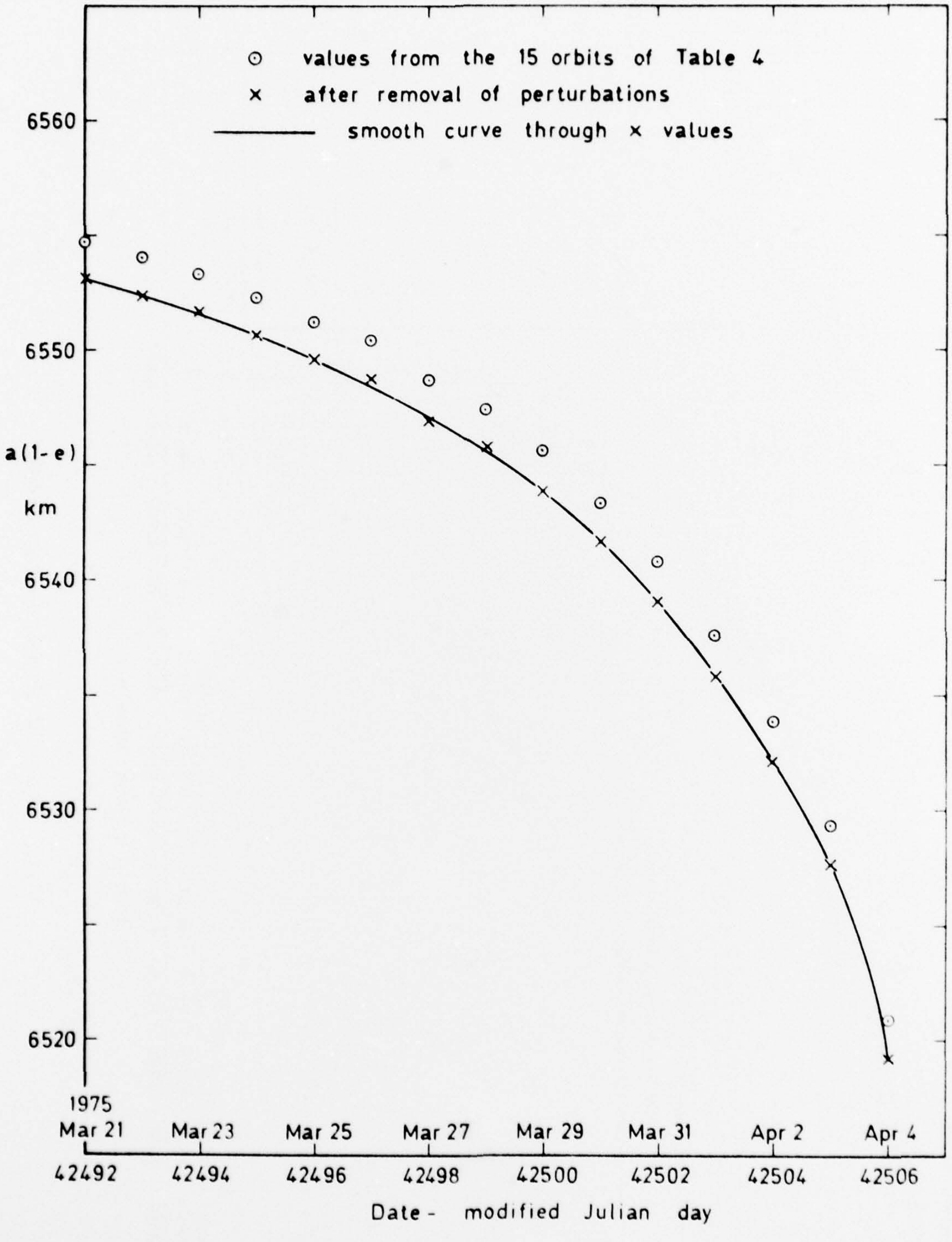

Fig 14 Variation of a(1 − e) for last 15 days

TR 78089

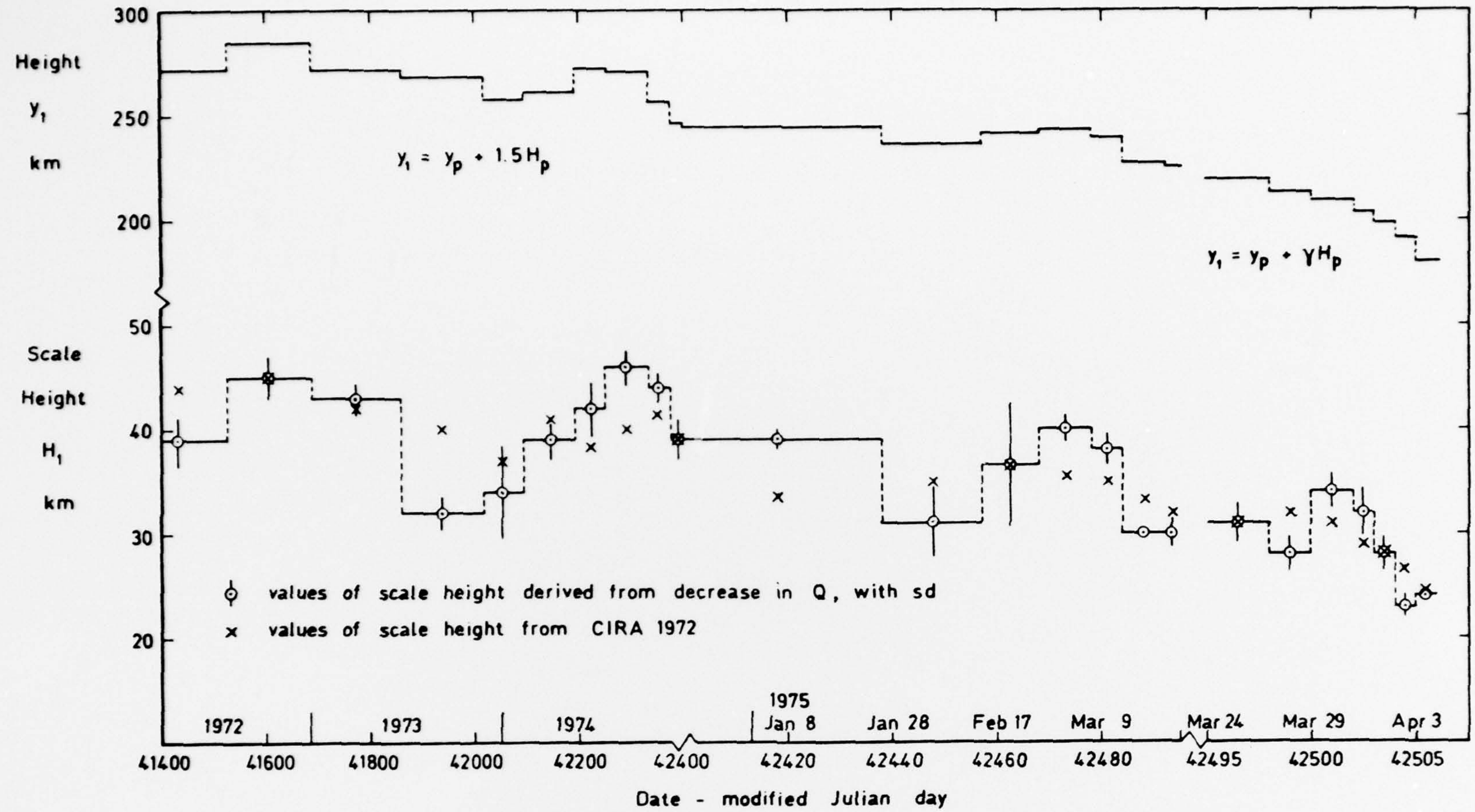

Fig 15 Values of density scale height H_1 at height y_1 for 1972–1975